University of Stavanger

FACULTY OF SCIENCE AND TECHNOLOGY

MASTER'S THESIS

Study program/specialization: Master of Science in Petroleum Engineering. Specialization-Reservoir Engineering.	Spring semester, 2018. Open / Confidential
Author: Carlos Ramirez Pacheco	…… (signature of author)
Supervisor(s): Professor Jann Rune Ursin	
Title of master's thesis: **STOCHASTIC THERMODYNAMIC PRODUCTION MODEL FOR SHALE GAS RESERVOIRS.**	
Credits:30	
Keywords: Stochastic, Spherical, Diffusion, Thermodynamic, Production, Model, Shale, Gas, Reservoirs, Adsorption, Desorption, isotherm, Forecast, ST PRO Model, Reservoir Engineering, Method, Area, Quantification	Number of pages: 52 Stavanger, 15.06.2018 Date/year

Abstract.

Most operating companies use Decline Curve Analysis (DCA) for their production forecast on Shale Gas assets (Mongalvy, Chaput and Agarwal, 2011). DCA method is based in empirical analysis and the theoretical background behind DCA for shale gas wells has not been fully proven. In addition to the DCA method, there are methods based in flow equations discretized using finite difference method (FDM). Currently, neither of these methods fully provide a physical thermodynamic description of the processes occurring at the reservoir. Also, none of the models by themselves provide a possible surface desorption area of the of the induced fracture network. This thesis contains a dedicated Stochastic Thermodynamic Production Model for Shale gas reservoirs (named ST Pro model) as a possible novel way of forecasting the production of shale gas wells. This novelty is by means of a stochastic thermodynamic analysis of the geochemical properties of shale gas.

The ST PRO Model assumes the free gas contained in the micro fractures flows at the initial production of the well. Once all free gas in the micro fractures has been released to the surface, the well performs uniquely based on the desorption production mechanism. The desorption is modeled by means of the geochemical characteristics of the shale gas combined with first and second law of thermodynamics. ST PRO Model uses an isotherm based on entropy (named RP isotherm) to model desorption. RP isotherm is proposed as an alternative to Langmuir or Freundlich adsorption isotherms. ST PRO Model provides a gas production forecasting of an individual well or group of wells located at a shale gas reservoir. Additionally to forecasting, ST PRO Model gives an estimation of desorption surface area from where the shale gas is desorbing into the well. This is by means of a spherical diffusion model inspired by John Crank's model. The original model was adapted to our specific process of shale gas desorption, and applied to quantify the surface area of the fracture network from where the shale gas might be desorbing at reservoir conditions.

ST PRO Model was applied in a group of wells located at Appalachian Basin, USA. ST PRO Model can potentially provide: 1) Production forecast of an individual or a group of wells; 2)A possible surface desorption area of the induced fracture network .

ST PRO Model is a potential novel tool for forecasting and surface desorption area quantification in an individual or group of shale gas wells. A new desorption isotherm based on entropy is proposed. Novel analysis is shown by means of a stochastic thermodynamic analysis of the geochemical properties of shale gas.

CONTENTS

LIST OF FIGURES.

Chapter 1: Introduction.

Most operating companies use Decline Curve Analysis (DCA) for their production forecasts on Shale Gas assets (Mongalvy, Chaput and Agarwal, 2011). DCA method is based on empirical analysis and the theoretical background behind DCA for shale gas wells has not been fully proven. In addition to the DCA method, there are numerical simulators based on flow equations discretized using the finite difference method (FDM) (Shaw and Stone, 2005) used in commercial reservoir simulators, such as Eclipse. In reference to desorption modelling, the DCA method does not consider any sorption isotherm processes during its formulation. Flow models based in FDM commonly employ the empirical Freundlich sorption isotherm or Langmuir sorption isotherm to represent physical phenomena during gas production from shale gas reservoirs.

These methods are frequently used to forecast gas production and to describe desorption from shale gas reservoirs. It seems neither method fully provides a physical thermodynamic description of the processes occurring in the reservoir. In addition, none of the models by themselves provide a possible surface desorption area of the of the induced fracture network. We understand induced fracture network as the network of fractures created during the hydraulic fracturing operation and the natural fractures exposed for desorption during a natural spontaneous production process behavior.

This thesis contains a dedicated Stochastic Thermodynamic Production Model for Shale gas reservoirs (named ST PRO Model) based in a novel way of forecasting shale gas wells. This novelty is by means of a thermodynamic analysis of the geochemical characteristics of shale gas and a stochastic spherical diffusion model. We assume the free gas contained in the micro fractures flows when the well starts production. Once all free gas in the micro fractures has been produced at the surface, we assume the well produces gas uniquely under a desorption mechanism. This model is applicable when the production of the well is fully driven by a desorption mechanism.

The objective for ST PRO Model is to provide a gas production forecasting method of an individual well or group of wells located at a shale gas reservoir and to quantify a possible desorption area of the induced fracture network.

ST PRO Model is composed of two parts: thermodynamic analysis of geochemical characteristics of shale gas and quantification of the most likely desorption area of the induced fracture network. In relation to the thermodynamic analysis, we will derive an isotherm based

on entropy (named RP isotherm) to model the adsorption/desorption process that occurs during the production of shale gas. RP isotherm is proposed as an alternative to Langmuir and Freundlich adsorption isotherms for adsorption/desorption processes. The second part of ST PRO Model quantifies the most likely desorption area of the induced fracture network by means of a stochastic spherical diffusion model. The stochastic spherical diffusion model has been inspired by the spherical diffusion model created by John Crank (John Crank reference). The original model has been adapted for our specific process of shale gas desorption. In ST PRO Model, a stochastic variable has been introduced to calculate the internal surface area of a sphere.

ST PRO Model has the workflow contained in figure 1.1.

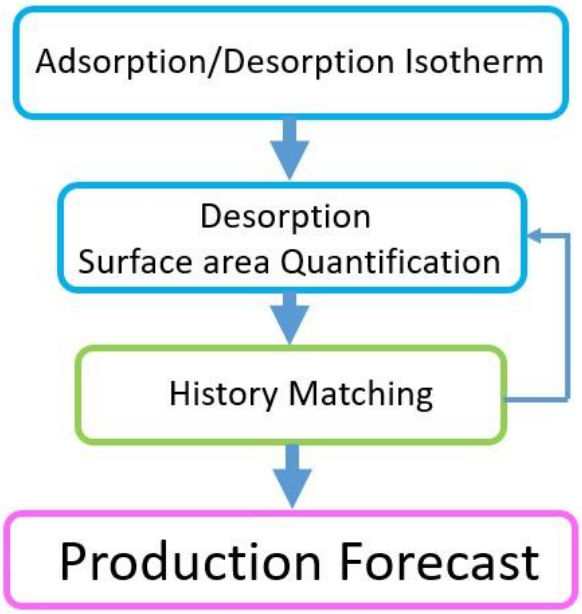

FIGURE 1.1. ST PRO Model Workflow

Chapter 2 contains a description of the main characteristics of shale gas reservoirs. Geochemical characteristics and thermal maturity are directly related to the fundamentals of the derivation of ST PRO Model.

Chapter 3 is dedicated to the adsorption/desorption thermodynamic analysis performed during shale gas production processes. It contains a conceptualization of the relationship between the

first and second law of thermodynamics during shale gas production processes. RP adsorption/desorption isotherm is derived at the end of the chapter.

Chapter 4 derives and explains the desorption surface area by utilizing a stochastic spherical diffusion model. Initially, we will provide the original model derived by John Crank and give a general description of the parts which conform to the model. Subsequently, we will derive a stochastic spherical diffusion model to quantify the most likely desorption surface area. The desorption is quantified by a stochastic variable. Using a Monte Carlo simulation with one million iterations, the mean of the distribution we will obtain represents the most likely internal surface area.

Chapter 5 presents the results and discussions from a case study. The case study is a quadrangle of wells located at Sandy Field, Appalachian Basin (part of the Marcellus shale play) which are located East of Kentucky, USA. The case study will include an analysis and discussion of the results for each of the wells within their quadrangle and the entire quadrangle.

Chapter 6 contains the conclusions of the thesis.

Chapter 2: Characteristics of Shale Gas Reservoirs.

Shale gas reservoirs are different from conventional reservoirs in many respects. Shale gas reservoirs have multiple porosities, ultra-low permeability and the capacity to adsorb large quantities of gas. The objective of this chapter is to introduce shale gas reservoirs by giving their main characteristics as will be derived by the ST PRO Model.

2.1 Introduction to shale gas reservoirs.

Shale gas reservoirs are one of the most important unconventional gas resources. This importance is due to the enormous resource potential which has been proven, especially in the United States of America.

Shale gas reservoirs can have matrix permeability values in the range of tens to hundreds of nanodarcies. Three decades ago, shale gas was considered economically and technically unrecoverable. Today the extraction of gas from shale gas reservoirs is largely attributed to the introduction and maturation of two technologies: massive hydraulic fracturing and long reach horizontal wells(Sigal, Deepak and Civan, 2015). This has been significantly assisted by the high brittleness of shale plays such as Barnett shale(Wang and Reed, 2009). The extraction of gas from other shale gas plays in the US (such as Marcellus, Fayetteville, Haynesville, Antrim and New Albany) followed similar trends (EIA, 2018).

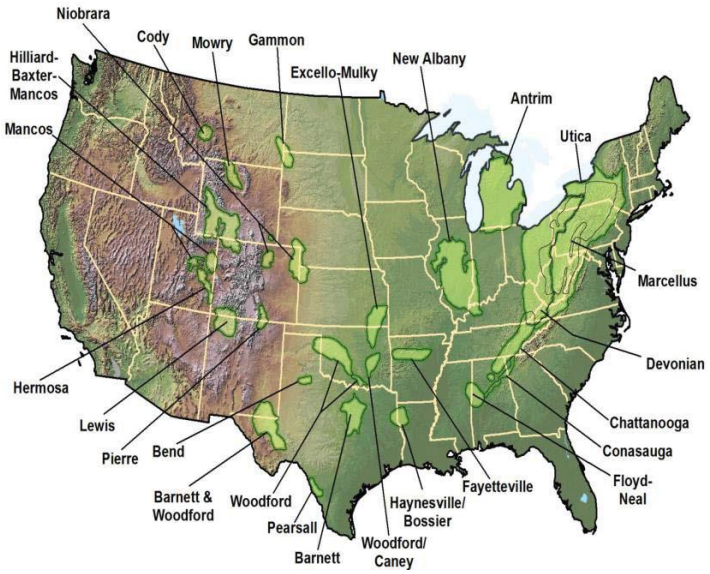

FIGURE 2-1 Major Shale gas basins, report published by US DOE.

In the USA, the production of shale gas is expected to increase considerably the production in the future. According to the EIA Annual energy Outlook 2018, the gas production from shale gas reservoirs will increase from the current 15 TCF to 33 TFC in 2050(EIA, 2018). Figure 2.3 shows previous and estimated production forecasts of natural gas production in the USA.

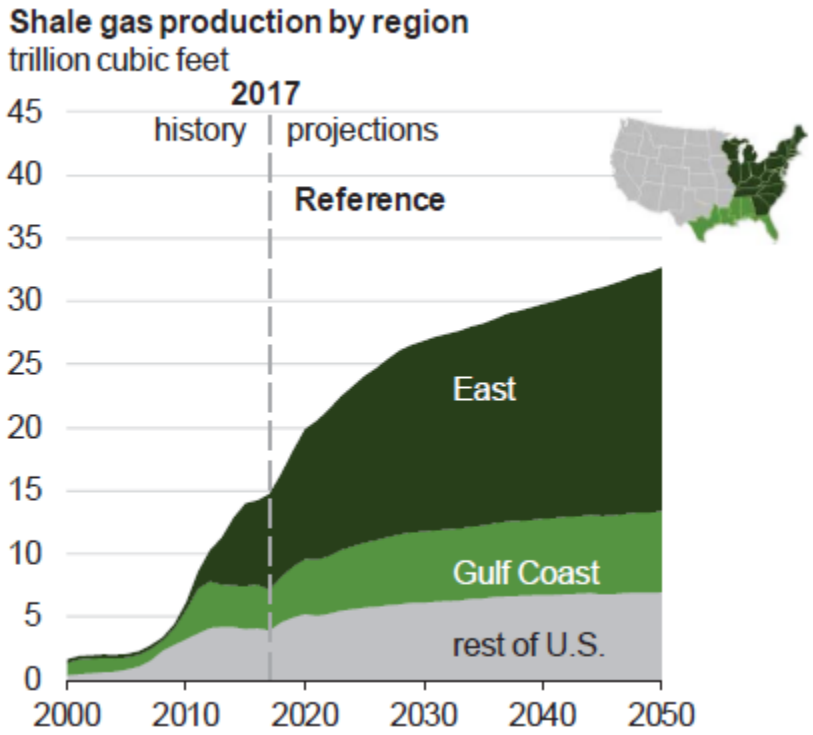

FIGURE 2.2 Historical and forecasted US natural gas production by region. EIA, 2018.

Shale gas reservoirs have mainly been developed in the USA, but there is considerable potential for shale gas production globally, as can be seen from figure 2-2.

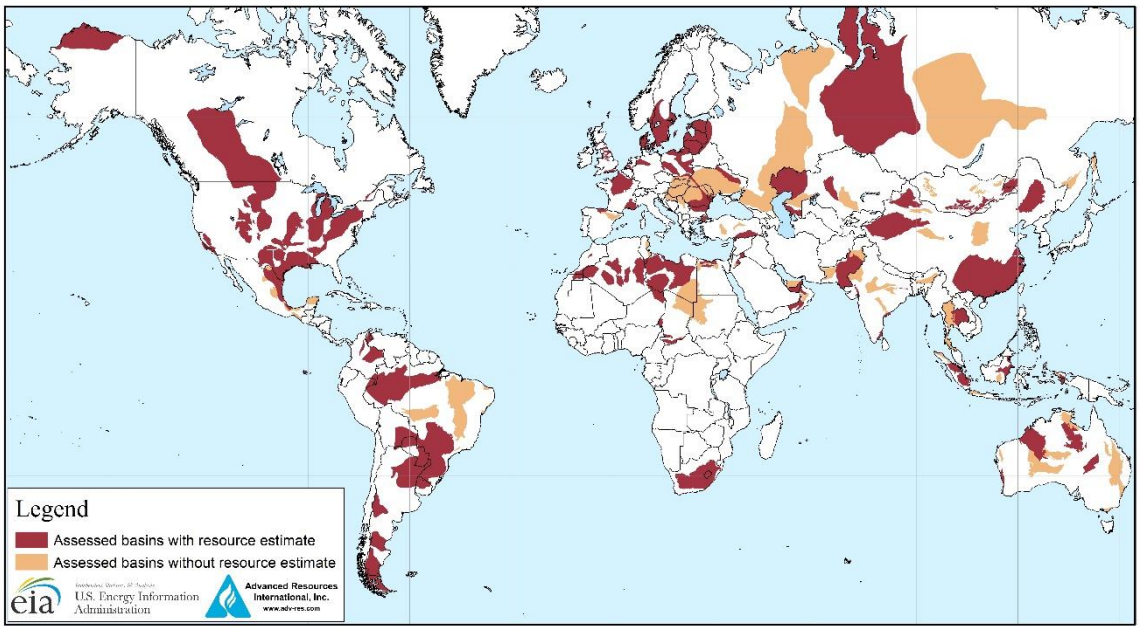

FIGURE 2-3 Assessed resource basin map(EIA, 2018).

2.2 Multiple porosities.

In a shale gas producing system, we can infer there are four types of porosities: inorganic porosity, organic porosity, natural micro-fractures and porosity created artificially by hydraulic fracturing.

Inorganic porosity (kerogen porosity) and organic porosity (bitumen porosity) are related to geochemical characteristics of shale gas reservoirs.

Natural networks of microfractures are considered to be important during shale gas production. The porosity of those networks is considered to be less than 0.5%, and it is hypothesized they have significant fluid conductivity. This porosity results in higher than expected gas production rates in shale gas reservoirs (Wang and Reed, 2009).

2.3 Ultra low permeability.

Many shale gas and ultra-low permeability tight gas reservoirs can have matrix permeability values in the range of tens to hundreds of nanodarcies(Swami, Clarkson and Settari, 2012). These type of reservoirs are challenging in terms of Production and Reservoir engineering. For Production Engineering, the challenge of extracting gas from shale gas reservoirs stems from the fact that ultra-low permeability does not allow the wells to produce at profitable levels without stimulation. For Reservoir Engineering, the challenge is that the ultra-fine pore structure of these rocks violates the basic assumptions behind the application of Darcy's law. (Swami, Clarkson and Settari, 2012). In order to model the physical phenomena of shale gas resources, there are different models to describe transport physics behind a non-Darcy shale gas producing wells. Most of the models involve applying to Knudsen diffusion theory or Langmuir adsorption isotherm. ST PRO Model represents an alternative method to model gas production from shale gas reservoirs.

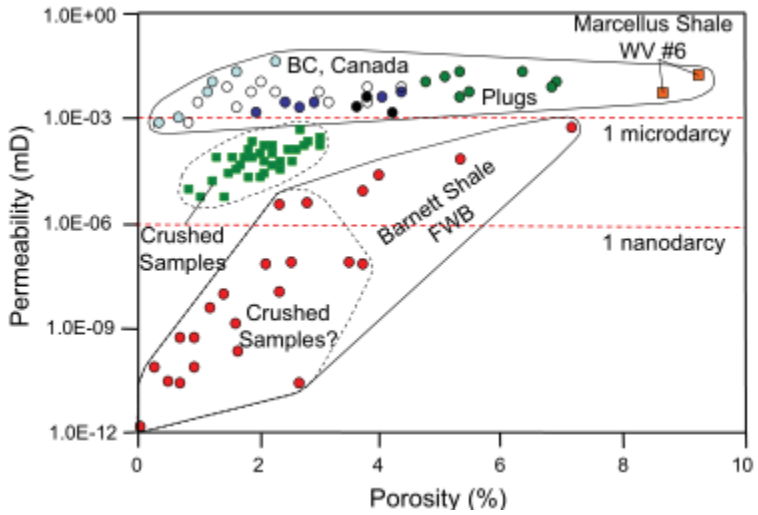

FIGURE 2.4 Porosity and permeability relationships experienced in North American shale plays (Wang and Reed, 2009).

2.4 Geochemical characteristics of shale gas reservoirs.

Shale gas systems are petroleum-source rocks. These rocks consist of organic matter from which petroleum is generated. Rock matrix consists primarily of clays, silicates, and carbonates in varying proportions. (Jarvie, 2015) and organic matter is a minor constituent of the total rock matrix. This organic matter is converted into petroleum upon increasing its temperature. Sources of heat include: heat from the mantle, hydrothermal heating or heating by radioactive decay). (Jarvie, 2015). Insoluble organic matter, also known as kerogen, is formed at temperatures below 90°. Petroleum generation occurs between a temperature range of about 90-120(Jarvie, 2015).

The principal source of hydrocarbons is derived from decomposition of soluble bitumen(Behar and Jarvie, 2013), the primary product of kerogen cracking. It has been proven that kerogen yields less than 35% of the hydrocarbons and that bitumen cracking yields the remainder of hydrocarbons generated(Jarvie, 2015).

One of the most important determinants of the volume of gas that can be generated is the relative quantity and quality of organic matter preserved from the deposited biomass. To measure this, the total organic carbon(TOC) has to be measured and recorded by its weight percent of organic carbon in the rock matrix. Usually the volume of the rock occupied by TOC is approximately double the weight percent due to its low density in comparison to the inorganic rock matrix(Jarvie, 2015).

Knowing the TOC and relative hydrogen contents is the essential to evaluate the overall petroleum generation potential. In addition to this information, we need to obtain the maximum temperature that the reservoir was exposed to. We can refer to this maximum temperature as Thermal Maturity. Thermal Maturity is used to describe the organic matter decomposition as being in the oil or gas window(Jarvie, 2015). The fluid to be produced from the reservoir, oil or gas, depends of the thermal maturity of the reservoir. It seems gas is produced from reservoirs with higher TOC and temperature than in the oil cases. In order to measure the Thermal Maturity of the reservoir, the vitrinite reflectation must be measured. Vitrinite is an organoclast derived from catagenetically altered woody plat tissues. Vitrinite reflectance indicates the maximum paleo-temperature to which the sediment has been exposed to (Jarvie, 2015). This temperature is usually different from the bottom-hole temperature as a result of the sediments generally being deeply buried and subsequently heated to lower temperatures.

It is important to remark that in previous experiments and empirical results, it seems that an excess of thermal maturity reduces the amount of gas in shale gas reservoirs. This reduction is physically demonstrated as a negligible amount of gas, even when the reservoir has characteristics of a shale gas producing well. This is hypothesized to be due to oxidation of methane, but may be also due to destruction of the porosity in the rock fabric and the subsequent loss of retained gas (Jarvie, 2015).

Chapter 3: Adsorption/desorption of Shale gas as a thermodynamic process.

Chapter 3 is dedicated to modeling the adsorption/desorption process in a shale gas reservoir. The model has been derived from thermodynamic analysis of the geochemical properties of shale gas. Initially we will explain the thermodynamic concepts of state and simple equilibrium in a shale gas reservoir. Afterwards, we will relate the geochemical characteristics of shale gas with the *first and second law of thermodynamics* during a shale gas production process. At the end, we will derive an isothermal adsorption/desorption equation which allows us to model adsorption/desorption by means of entropy. We named the adsorption/desorption isotherm based in entropy as "RP isotherm".

3.1 Concept of state in a shale gas production process.

The concept of *state* in thermodynamics is defined from two different perspectives: microscopic state and macroscopic state. The microscopic state relates to the measurement of masses velocities, positions and modes of motion of all of the constituent particles of a system. As this detailed information is unlikely to be known in a shale gas production process, we need to determine the state of the system from a different perspective. This different perspective is named macroscopic state of the system and refers to the properties which can be measured from a macroscopic point of view. These properties capable of being measured are mainly pressure, volume and temperature. In order to fix the state of the system, only two properties have to be known, and the rest will be automatically fixed (Gaskell, 2003). These two fixed properties can be known as the independent properties and the rest as dependent properties.

In a shale gas well at initial conditions, we will assume a fixed amount of producible volume of gas (V), initial pressure (P) and temperature (T). The fixed volume of gas can be referred to as the total recoverable volume of gas. The mathematical relationship between V, P and T for the initial system can be expressed as an equation of state for that specific system. In a three-dimensional diagram, with coordinates representing temperature, volume and pressure, all the points P-V-T where the system is in equilibrium, generate a surface. This is shown in figure 3.1.

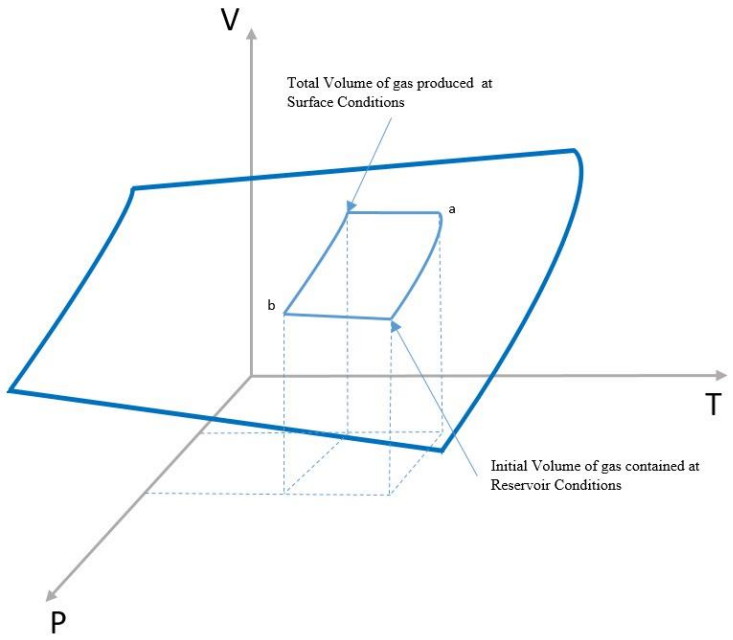

FIGURE 3.1 Over the surface represented in the figure 3.1, all the points are in equilibrium.

We assume the process will have a constant volume if the initial volume of producible gas is equal to the volume of gas to be produced at surface conditions. Currently, it is unlikely we can establish the exact volume of gas that is contained in the reservoir and which can be producible by the well at initial reservoir conditions. In any case, we can measure the production at surface conditions and use the total cumulative production of shale gas at surface conditions as a source of information. This information will lead us into a final state. The final state is also known as the total volume of gas recoverable at surface conditions. The previous idea is the foundation of the ST PRO Model. To simplify terminology in further sections of this thesis, we will refer to the total volume of gas produced at surface conditions as Final State, and the total volume of producible gas at reservoir conditions is named as Initial State. As we saw before, by fixing the two independent variables the third variable will automatically be fixed. During the process, assuming pressure and temperature at initial constant conditions and final constant conditions, the change in volume of shale gas can be expressed by this equation:

$$\Delta V = V_{reservoir} - V_{surface} \quad (3.1)$$

As we can see in figure 3.1, the process can take an infinite number of paths in a PVT diagram. Certainly, the path the gas takes during the production is not relevant for this study, and we will focus more on the Initial State (original gas reserves) and Final State (total gas recovery). In any case, we will need an expression to represent the change in volume by moving the shale gas from its Initial State to a Final State.

Even when the process of producing shale gas from initial reservoir conditions to final surface conditions at constant volume can take an infinite number of paths, we can pick two possible paths and call them path “a” and path “b”: Reservoir→a→Surface and Reservoir→b→Surface. Starting with the path Reservoir→a→Surface, the change in volume can be represented as:

$$\Delta V = V_{reservoir} - V_{surface} \dots \dots \dots \dots \dots \dots \dots \dots \dots \dots \dots \dots \dots \dots \dots \dots \dots \dots \dots \dots \dots \dots \dots \dots \dots \dots \dots . (3.2)$$

$$\Delta V = \left(V_a - V_{surface}\right) + \left(V_{reservoir} - V_a\right) \dots \dots \dots \dots \dots \dots \dots \dots \dots \dots \dots \dots \dots \dots \dots \dots \dots \dots \dots \dots (3.3)$$

By considering this path, the process from reservoir→a occurs at constant Pressure $P_{surface}$ and process a→Surface at constant temperature $T_{reservoir}$:

$$\left(V_a - V_{surface}\right) = \int_{T_{surface}}^{T_{reservoir}} \left(\frac{\partial V}{\partial T}\right)_{P_{surface}} dT \dots \dots \dots \dots \dots \dots \dots \dots \dots \dots \dots \dots \dots \dots \dots \dots \dots \dots (3.4)$$

And

$$\left(V_{reservoir} - V_a\right) = \int_{P_{surface}}^{P_{reservoir}} \left(\frac{\partial V}{\partial P}\right)_{T_{reservoir}} dP \dots \dots \dots \dots \dots \dots \dots \dots \dots \dots \dots \dots \dots \dots \dots \dots \dots . (3.5)$$

Thus

$$\Delta V = \int_{T_{surface}}^{T_{reservoir}} \left(\frac{\partial V}{\partial T}\right)_{P_{surface}} dT + \int_{P_{surface}}^{P_{reservoir}} \left(\frac{\partial V}{\partial P}\right)_{T_{reservoir}} dP \dots \dots \dots \dots \dots \dots \dots \dots \dots \dots (3.6)$$

Applying the same to the path Reservoir→a→Surface

$$\left(V_b - V_{surface}\right) = \int_{T_{surface}}^{T_{reservoir}} \left(\frac{\partial V}{\partial P}\right)_{T_{surface}} dP \dots \dots \dots \dots \dots \dots \dots \dots \dots \dots \dots \dots \dots \dots \dots \dots \dots \dots (3.7)$$

$$\left(V_{reservoir} - V_b\right) = \int_{T_{surface}}^{T_{reservoir}} \left(\frac{\partial V}{\partial T}\right)_{P_{reservoir}} dT \dots \dots \dots \dots \dots \dots \dots \dots \dots \dots \dots \dots \dots \dots \dots \dots \dots . (3.8)$$

$$\Delta V = \int_{P_{surface}}^{P_{reservoir}} \left(\frac{\partial V}{\partial P}\right)_{T_{surface}} dP + \int_{T_{surface}}^{T_{reservoir}} \left(\frac{\partial V}{\partial T}\right)_{P_{reservoir}} dT \ldots\ldots\ldots\ldots\ldots\ldots\ldots\ldots\ldots\ldots (3.9)$$

As a conclusion, we can assume that the volume of gas from initial reservoir conditions to final surface conditions can be infinitesimal, and independently of the path taken, they still having the same initial volume at initial reservoir conditions and final volume at final surface conditions.

$$dV = \left(\frac{\partial V}{\partial P}\right)_T dP + \left(\frac{\partial V}{\partial T}\right)_P dT \ldots\ldots\ldots\ldots\ldots\ldots\ldots\ldots\ldots\ldots\ldots\ldots\ldots\ldots\ldots\ldots\ldots\ldots\ldots\ldots\ldots\ldots\ldots\ldots (3.10)$$

3.2 Concept of simple equilibrium in a shale gas production process.

Simple equilibrium occurs exclusively at initial conditions and final conditions. At initial conditions, we assumed a fixed volume of producible gas at initial reservoir conditions of pressure and temperature. At final conditions, we refer to the total volume of produced gas at surface conditions of pressure and temperature. This final state infers no more gas can be produced from the well by natural mechanisms. Figure 3.2 represents the two simple equilibriums assumed to occur during a shale gas production process.

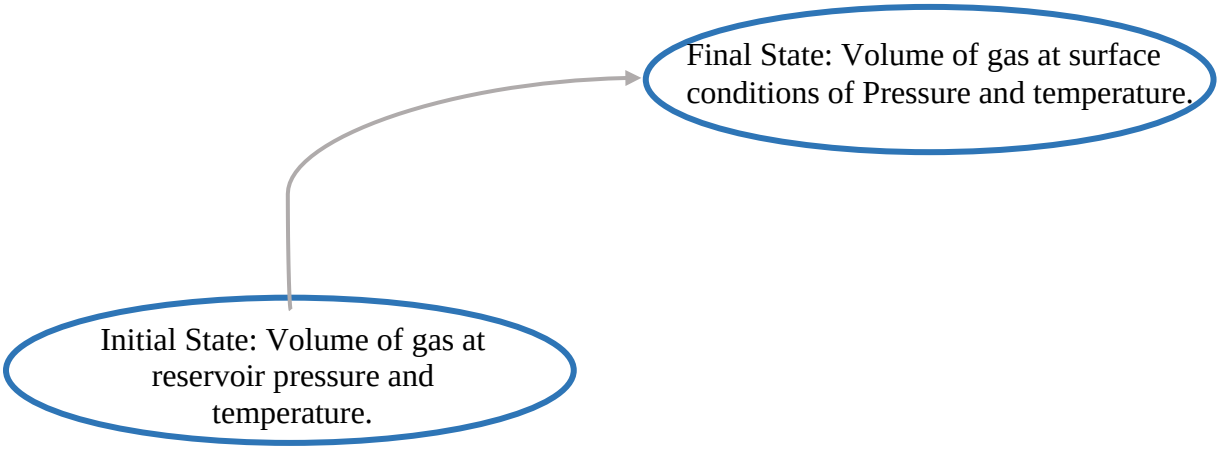

FIGURE 3.2 Simple Equilibrium states assumed to occur during a shale gas production process.

3.3 *First Law of Thermodynamics* during a shale gas production process.

In this section, we will discuss how *the first law of thermodynamics* can possibly be applied to a shale gas production process. We have made three main assumptions. The first assumption is based on a possible direct relationship between the concepts of thermal maturity and the quantity of heat adsorbed by the organic material in a shale gas play. As we saw in chapter 2, the concentration of gas in a shale gas play largely depends upon the thermal maturity of the reservoir. Also, when the organic material is exposed to a heat source, this might help to generate gas at reservoir conditions. The first assumption is that the heat is adsorbed by the organic material due to thermal exposure at reservoir conditions. A physical interpretation of the first assumption is that heat absorbed into organic material is generating gas in the reservoir. The second important assumption relates to the production of shale gas as a process where the expansion of gas will perform work. A third assumption is that the work performed by the expansion of gas is equivalent to the heat released by the gas as a reversible process. In the following sections, the reader will find a discussion to aid their understanding of the previous assumptions In this chapter, we assume that the system is a reversible process. The explanation of *reversibility* of the system is provided in the section dedicated to *second law of thermodynamics* during the production of shale gas reservoirs.

3.3.a Relationship between heat and work as a shale gas production process.

According to the research conducted on geochemical properties of the shale gas plays, reservoirs with a higher Maturity Temperature might contain larger amounts of gas than oil. ST PRO Model assumes a reservoir with a maturity temperature that is high enough to let the well exclusively produce gas and, simultaneously, a Maturity Temperature that is low enough so that gas can effectively be produced. When a well is open for production, we can say the work performed by the gas is related to the expansion it suffers due to a change of pressure. The change of pressure is due to the pressure differential between the bottomhole pressure (BHP) of the wells once it is open for production, and the initial conditions of the reservoir. Simultaneously with the change of pressure, heat is released by the gas which is initially located at reservoir conditions into the well. Given we are considering a reversible cyclic system, heat and work will be equal during the whole process.

3.3.b Internal energy and *First Law of Thermodynamics.*

In a well producing gas from a shale gas formation, we assumed the change in the internal energy (U) of the system is a process which simultaneously performs work and release heat. The heat released "q" from the reservoir into the well and the work "w" performed by gas expansion during a production process can be represented mathematically as follows:

$$\Delta U = q - w \quad \ldots\ldots (3.11)$$

This statement leads to the *First Law of Thermodynamics* in our particular case.
For an infinitesimal change of state, equation (3.11) can be written as a differential equation:

$$dU = \delta q - \delta w \quad \ldots\ldots (3.12)$$

As U is a state function, the integration of dU between two states is independent of the path taken by the system. Figure 3.3 represents the independency of paths and states.

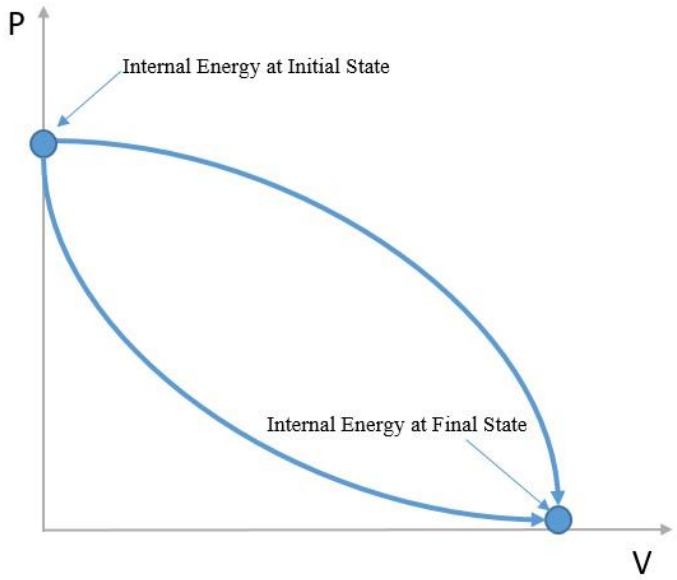

FIGURE 3.3 Graphical representation of independency of paths between an initial internal energy state and final internal energy state.

Now we will use the system's reversibility to demonstrate the independence of the paths from initial state and final state. The system's reversibility will be explained in more detail in the chapter dedicated to the *second law of thermodynamics*. In the case of a cyclic process, the system returns to its initial state and the internal energy U of the process is equal to zero.

$$\Delta U = \int_{Reservoir}^{Surface} dU + \int_{Surface}^{Reservoir} dU = \left(U_{surface} - U_{reservoir}\right) + \left(U_{reservoir} - U_{surface}\right) = 0. \quad (3.13)$$

The vanishing of a cyclic integral is a property of a state function.

$$\oint dU = 0 \ldots \ldots \ldots \ldots \ldots \ldots \ldots \ldots \ldots \ldots \ldots \ldots \ldots \ldots \ldots \ldots \ldots \ldots \ldots \ldots \ldots \ldots \ldots \ldots \ldots \ldots \ldots \ldots \ldots \ldots \ldots \ldots \ldots . (3.14)$$

Having demonstrated U as a state function, we will now consider a shale gas production system with a fixed amount of producible gas. The value of U can be fixed once two independent properties are fixed. We have chosen temperature T and volume V as independent variables:

$$U = U(V, T) \ldots \ldots \ldots \ldots \ldots \ldots \ldots \ldots \ldots \ldots \ldots \ldots \ldots \ldots \ldots \ldots \ldots \ldots \ldots \ldots \ldots \ldots \ldots \ldots \ldots \ldots \ldots \ldots \ldots \ldots \ldots \ldots (3.15)$$

The complete differential in terms of partial derivatives gives:

$$dU = \left(\frac{\partial U}{\partial V}\right)_T dV + \left(\frac{\partial U}{\partial V}\right)_V dT \ldots \ldots \ldots \ldots \ldots \ldots \ldots \ldots \ldots \ldots \ldots \ldots \ldots \ldots \ldots \ldots \ldots \ldots \ldots \ldots \ldots \ldots \ldots \ldots . (3.16)$$

This equation will be used further up in developing the RP adsorption/desorption isotherm.

3.4 *Second Law of thermodynamics* during a shale gas production process.

The shale gas reservoir at initial conditions will remain at original conditions unless an external agent creates a non-equilibrium state. It seems possible to consider a gas producer well as a non-equilibrium agent just after it has been opened for production. Once the well is producing, the system has the characteristics of a spontaneous process. The system reaches a new state of equilibrium at surface conditions once the well is no longer producing gas by natural mechanisms. In the following subsections, we will discuss the production process of shale gas in terms of *the second law of thermodynamics.*

3.4.a Entropy and reversibility of the system by means of quantification of the irreversibility in the reservoir.

It seems that while a shale gas well is producing, the process behaves spontaneously. During spontaneous behavior, the process can be considered as an irreversible one. Due to irreversibility, we can assume the energy undergoing the process is degraded. Consequently, it is possible to measure the extent of degradation, or degree of irreversibility, of the system.

The spontaneous behavior of the process increases entropy. This increase in entropy can be considered a measure of the degree of irreversibility of the process. Therefore, the degree of irreversibility can be estimated by using the *second law of thermodynamics:*

$$\Delta S = \frac{q}{T} \quad \ldots\ldots (3.17)$$

If we rewrite the equation 3.17 as:

$$q = \Delta S * T \quad \ldots\ldots (3.18)$$

Assuming constant temperature, we can see a direct relationship between the entropy of the system and the heat released. It seems that the point of maximum entropy is closely related to the maximum heat released by the system. By using the production of gas as a source of information, the maximum heat released by the system can be assumed to be the maximum recoverable volume of gas measured at surface conditions. If we know the final recovery of gas from a well or reservoir, we can associate the maximum point of entropy with the total cumulative production of gas. See figure 3.4.

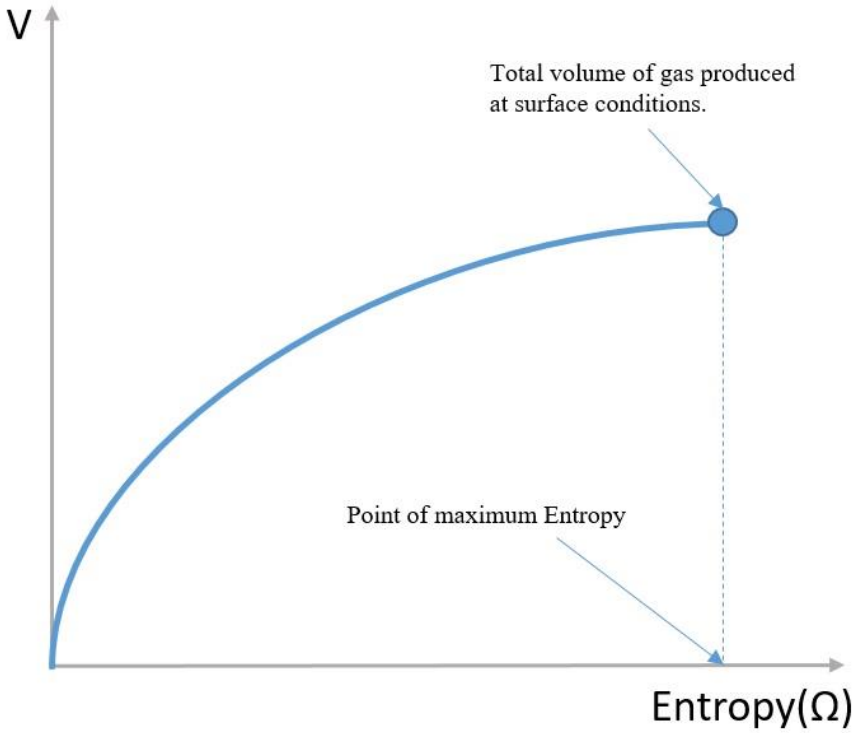

FIGURE 3.4 Maximum entropy associated with the known final recovery of gas.

If the well is currently producing, we can associate the current cumulative production as a pseudo final state and extrapolate the volume as a function of entropy in order to get the forecast by means of entropy. By extrapolating the entropy of the system, we will be able to find a possible final state of the system. The extrapolation of the final state of the system is shown in the figure 3.5.

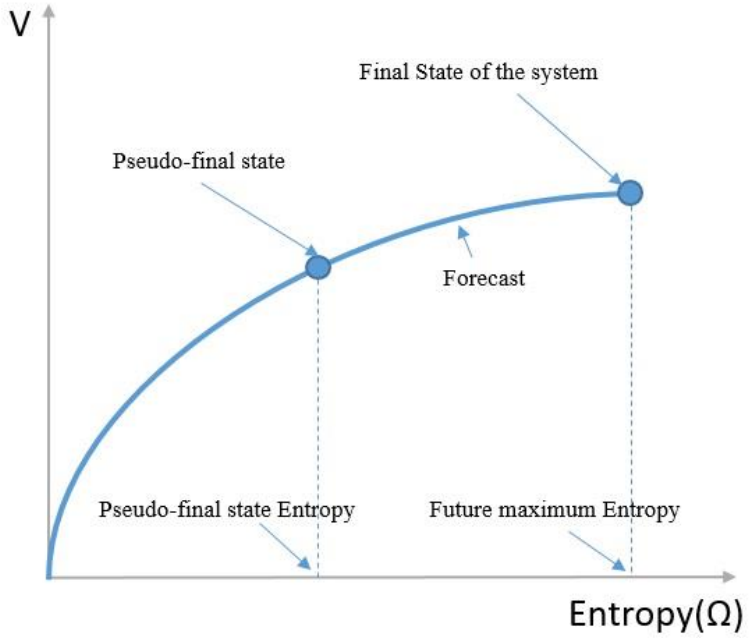

FIGURE 3.5 Pseudo final state used to forecast a possible final state by maximizing the entropy.

Once the system reaches its maximum entropy, it is ideally assumed that the system becomes a reversible process (See figure 3.6).

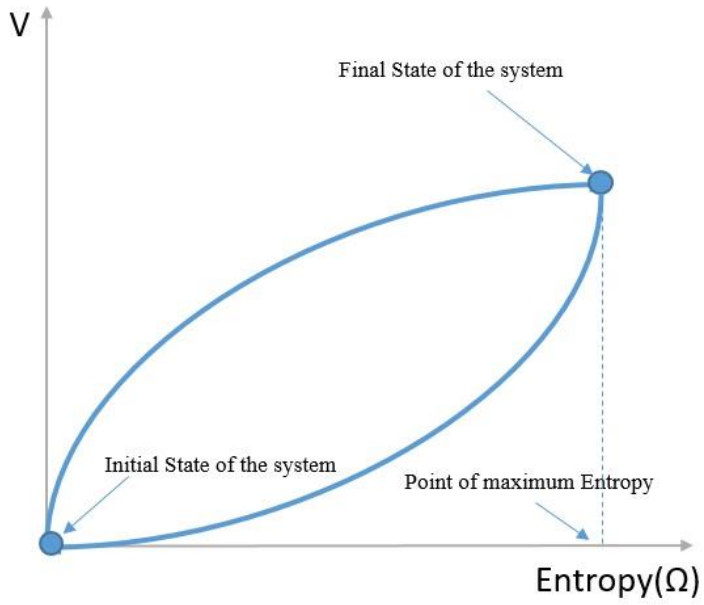

FIGURE 3.6 Idealization the system. At the point of maximum entropy, the system becomes a reversible process.

3.4.b Thermal equilibrium and the Boltzmann equation.

Considering a system of particles of shale gas in thermal equilibrium with a heat source at reservoir conditions. Now we let the state of the combined systems(shale gas particles + heat source) be fixed by fixing the values of U, V and n, where

$$U = U_{particles\ of\ gas} + U_{heat\ source}$$

$$V = V_{particles\ of\ gas} + V_{heat\ source}$$

n=number of particles in the system + the heat bath of fixed size.

As the particles system and the heat bath are in thermal equilibrium, small exchanges of energy can occur between them, and for such a small exchange at constant U,V, and n, the equation for the particles system is(Gaskell, 2003).

$$\delta In\ \Omega = \frac{\delta U}{K_b T} \dots\dots\dots\dots\dots\dots\dots\dots\dots\dots\dots\dots\dots\dots (3.19)$$

As this exchange of energy is carried out at constant total volume, then

$$\delta U = \delta q \dots\dots\dots\dots\dots\dots\dots\dots\dots\dots\dots\dots\dots\dots (3.20)$$

Also assuming the energy exchange occurs as an exchange of heat:

$$\delta In\ \Omega = \frac{\delta q}{K_b T} \dots\dots\dots\dots\dots\dots\dots\dots\dots\dots\dots\dots\dots\dots (3.21)$$

As the exchange of heat occurs at constant temperature, and occurs reversibility, then, we can use *the second law of thermodynamics*

$$\frac{\delta q}{T} = \delta S \dots\dots\dots\dots\dots\dots\dots\dots\dots\dots\dots\dots\dots\dots (3.22)$$

And thus

$$\delta S = K_b \delta In\ \Omega \dots\dots\dots\dots\dots\dots\dots\dots\dots\dots\dots\dots\dots\dots (3.23)$$

As both S and Ω are state functions, the above expression can be written as a differential equation; integration of which gives:

$$S = K_b In\, \Omega \quad \text{… …} \quad (3.24)$$

The equation above is known as a Boltzmann equation(Gaskell, 2003).

3.5 RP adsorption/desorption isotherm.

In this section, we will connect the ideas from previous sections in this chapter and derive an expression to be used as an adsorption/desorption isotherm. We named it as "RP isotherm".
For an incremental change in the state of a closed system, the first law of thermodynamics gives equation 3.12:

$$dU = \delta q - \delta w \quad \text{… …} \quad (3.12)$$

Having a reversible process, the second law of thermodynamics equation (3.22) give us:

$dS = \frac{\delta q_{rev}}{T}$ or $\delta q = TdS$

and

$$\delta w = PdV \quad \text{… …} \quad (3.25)$$

Combining the two laws:

$$dU = TdS - PdV \quad \text{… …} \quad (3.26)$$

Rearranging

$$dS = \frac{dU}{T} dS - \frac{PdV}{T} \quad \text{… …} \quad (3.27)$$

Considering S as a dependent variable and U and V as independent variables

S=S(U,T)……………………………………………………………………………(3.28)

we obtain:

$$dS = \left(\frac{\delta S}{\delta U}\right)_V dU + \left(\frac{\delta S}{\delta V}\right)_U dV \ldots\ldots(3.29)$$

Comparing equation 3.27 with 3.29:

$$\left(\frac{\partial S}{\partial V}\right)_U = \frac{P}{T} \ldots\ldots(3.30)$$

Considering constant internal energy (U), constant temperature (T) and constant pressure (P). Rewriting the equation (3):

$$\frac{\mathrm{d}S}{\mathrm{d}V} = \frac{P}{T} \ldots\ldots(3.31)$$

we get:

$$\int_{S_0}^{S} Sds = \frac{P}{T}\int_{Vo}^{V} V \ldots\ldots(3.32)$$

By solving the integral:

$$S - S_0 = \frac{P}{T}(V - V_0) \ldots\ldots(3.33)$$

Assuming initial conditions as S_0 and V_0 = 0:

$$S = \frac{P}{T}V \ldots\ldots(3.34)$$

$$V = \frac{ST}{P} \ldots\ldots(3.35)$$

By using Boltzmann's equation (3.24) :

$S = K_b ln(\Omega)$

Substituting the Boltzmann entropy equation into equation (3.35):

$$V = \frac{K_b ln(\Omega)\, T}{P} \dots \dots \dots \dots \dots \dots \dots \dots \dots \dots \dots \dots \dots \dots \dots \dots \dots \dots \dots \dots \dots \dots \dots \dots \dots \dots \dots \dots \dots \dots .. (3.36)$$

By inferring P, T and n as constant values, given they do not change during the reversible process, we obtain the equation below

$$V = K_{RP}\ In(\Omega) \dots \dots \dots \dots \dots \dots \dots \dots \dots \dots \dots \dots \dots \dots \dots \dots \dots \dots \dots \dots \dots \dots \dots \dots \dots \dots \dots \dots \dots \dots \dots (3.37)$$

which is named as *RP isotherm* for adsorption/desorption applications.

Where:

$$K_{RP} = \frac{nK_b T}{P} \dots \dots \dots \dots \dots \dots \dots \dots \dots \dots \dots \dots \dots \dots \dots \dots \dots \dots \dots \dots \dots \dots \dots \dots \dots \dots \dots \dots \dots \dots \dots \dots (3.38)$$

The constant is named *RP constant* for adsorption/desorption applications.

Chapter 4: Stochastic spherical diffusion model for estimating a spherical desorption surface area.

This chapter contains the stochastic spherical diffusion model used to estimate the desorption surface area in the induced fractured network of a gas well producing from a shale gas reservoir (see figure 4.1). The stochastic spherical diffusion model has been inspired by the spherical diffusion model created by John Crank (Crank, 1975). We adapted the original model for the case of a stochastic reversible steady state process.

The original equation developed by John Crank is as follows:

$$Q = 4\pi Dt\left(\frac{ab}{b-a}\right)(C_2 - C_1) \quad \text{.....(4.1)}$$

In order to easily understand the following sections, we will refer to the terms included in this equation as:

- Diffusion term.
- Term dedicated to randomization of the radius of a sphere.
- Concentration.

In the following subsections, each term is explained and adapted to estimate the most likely internal surface area of a sphere with a given radius. By doing this adaptation, the model will be able to provide an estimate of the surface area from where the shale gas is desorbing into the induced fractured system of the well.

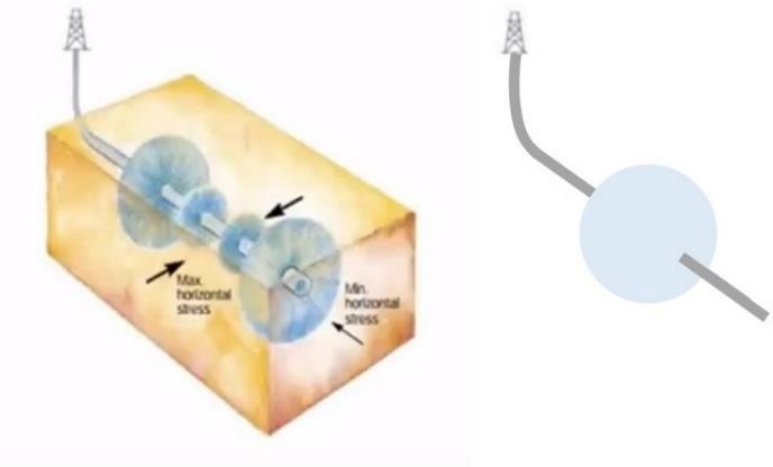

FIGURE 4.1 Left: Multi-stage Shale gas well (King, 2012). Right: ST PRO Model spherical desorption surface area of a well producing gas from a shale gas reservoir.

4.1 Random variable generator for calculation of the internal surface area of a sphere with radius “b” over a range (0,b).

In this subsection, we will derive an equation which calculates the surface area of a sphere in terms of the internal and external boundaries. By defining the surface area of a sphere in terms of the internal and external boundaries, we will be able to use the external boundary as a fixed boundary and the internal boundary as a stochastic variable. The external boundary is set to be a constant value and the internal stochastic boundary can give us an estimation of the most likely area inside the sphere.

First, we will derive an expression which calculates the surface area of a sphere in terms of an internal and external boundary. The internal boundary is named “a” and the external boundary “b”.

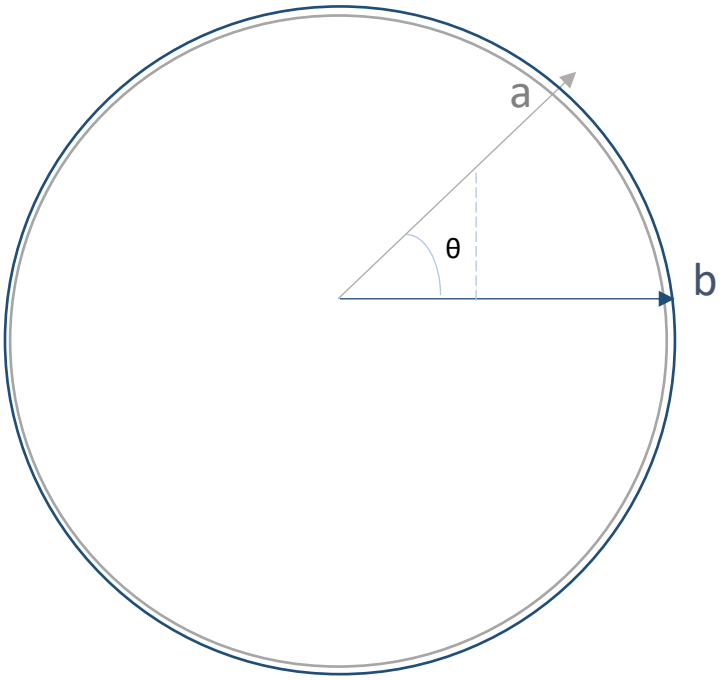

FIGURE 4.2. Graphical definition of the terms used for the calculation of the surface area of a sphere in terms of the internal and external boundaries. “a” represents the internal boundary. “b” represents the external boundary.

Considering:

$c = 2\pi b\ ; s = b\theta; ds = bd\theta$……(4.2)

Then,

$Surface_{sphere} = \int dA = \int 2\pi(acos\theta)bd\theta$ ……(4.3)

we integrate,

$Surface_{sphere} = 2\pi ab \int_0^{\frac{\pi}{2}} cos\theta d\theta \ * 2 = \ 4ab \ \int_0^{\frac{\pi}{2}} cos\theta d\theta$ ……(4.4)

evaluate:

$Surface_{sphere} = 4\pi ab \left[\sin\left(\frac{\pi}{2}\right) - \sin(0)\right]$ ……..(4.5)

At the end, we get the expression to calculate the surface of a sphere in terms of an internal and external boundary.

$Surface_{sphere} = 4\pi ab$ ……(4.6)

We consider the internal boundary “a” as a stochastic variable with a uniform distribution running over the range (o,b). The external boundary “b” is a constant value.

We will apply a random variable generator (RVG) to the expression which calculates the most likely internal surface area inside a sphere of fixed outer boundary value “b”. The most likely internal surface area inside the sphere is assumed to be the surface from where the shale gas is desorbing.

The external boundary will increase each iteration of the ST PRO Model until the historical data is matched(see fig. 1.1).

RVG=$\frac{ab}{b-a}$ ……(4.7)

RVG was solved by using Monte Carlo method. The flow diagram used for the Monte Carlo simulation is shown in the figure 4.3.

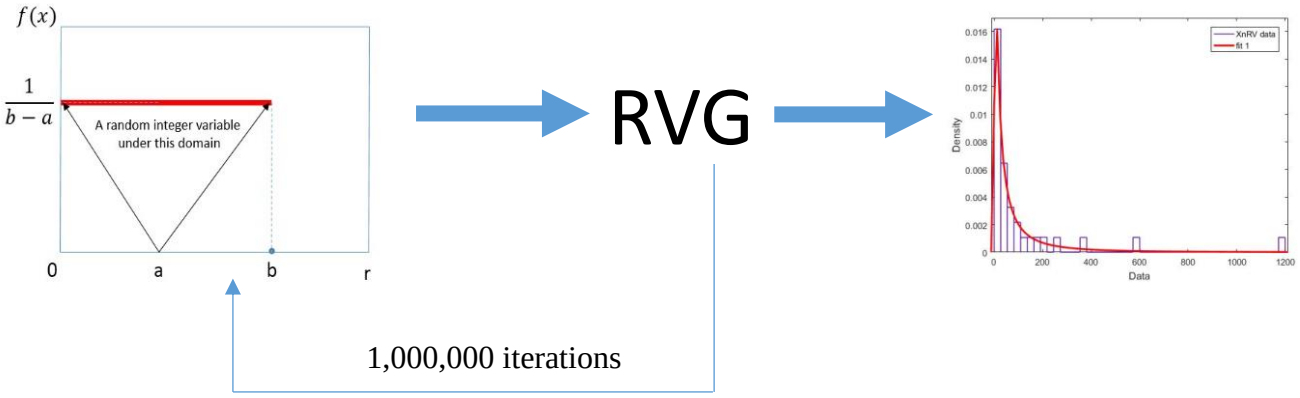

FIGURE 4.3. Flow diagram used for the Monte Carlo simulation.

The mean value of the logarithmic distribution obtained after the Monte Carlo simulation, represents the radius squared of a sphere whose area can be considered the desorption area from where the shale gas is desorbing into the induced fractured network of the well.

4.2 Diffusion in a reversible process.

Diffusion can be understood as the net movement of molecules or atoms from a region of high concentration to a region of low concentration because of the random motion of molecules and atoms. As it is random, it only applies for non-reversible spontaneous processes. ST PRO Model is assuming a state of maximum entropy in a reversible process, so the concept of diffusion as a random process is no longer possible. Diffusion has to take the value of one in order to make the process reversible. The last statement can be mathematically proven by the following theorem (Voß, 2004):

Let b: $R^d \rightarrow R^d$ be Lipschitz continuous, B a Brownian motion variable with vaues in R^d, and X a solution of the SDE:

$$dX = b(X)dt + dB \qquad \text{.....(4.8)}$$

With $X_0 \in L^2$. Then the following conditions are equivalent:

1) The process X is reversible with stationary distribution μ.
2) There is a function $\varphi: R^d \rightarrow R \; with \; b = -\nabla\varphi$ and $d\mu = \exp\big(-2\varphi(x)\big)\, dx$

$$\int_{R^d} \exp\big(-2\varphi(x)\big)\, dx = 1 \qquad \text{.....(4.9)}$$

4.3 Volume concentration of shale gas.

In the equation developed by John Crack uses a gradient concentration. In order to apply the equation to our specific case we will use a volume concentration.

$$\varphi_t = \frac{V_t}{V_F} = \frac{C_t}{C_F} \qquad \text{.....(4.10)}$$

By using a volume concentration, we will be able to obtain an adimensional concentration profile of the volume of gas produced during the life of the well or group of wells producing from a shale gas reservoir.

4.4 Stochastic Spherical Diffusion model for most likely internal surface area quantification.

By connecting the concepts explained in the previous subsections, we arrived at the following expression:

$$Q_i = 4\pi D \left(\frac{ab}{b-a}\right) \varphi_t \qquad \text{.....(4.11)}$$

Equation 4.11 is used by ST PRO Model to calculate a spherical surface desorption area.

Chapter 5: Case study using ST PRO Model.

In this chapter, we present a discussion of the analysis of the results of using real production gas shale data in the ST PRO Model. The results include forecast and most likely value of spherical desorption surface area for four individual wells and for a group of three and nine wells. All wells belong to the quadrangle Appalachi located at Appalachian Basin. East of Kentucky, USA. Quadrangle Appalachi is part of Sandy field. Sandy Field is located at the organic-rich Marcellus shale play, a significant hydrocarbon producer in the Appalachian basin. In 2012, a total of more than 21000 wells have been drilled in the Big Sandy field in east of Kentucky, southern West Virginia, southern Ohio, and southern Virginia(Zagorzy, Wrighstone and Bowman, 2012). See figure 5.1.

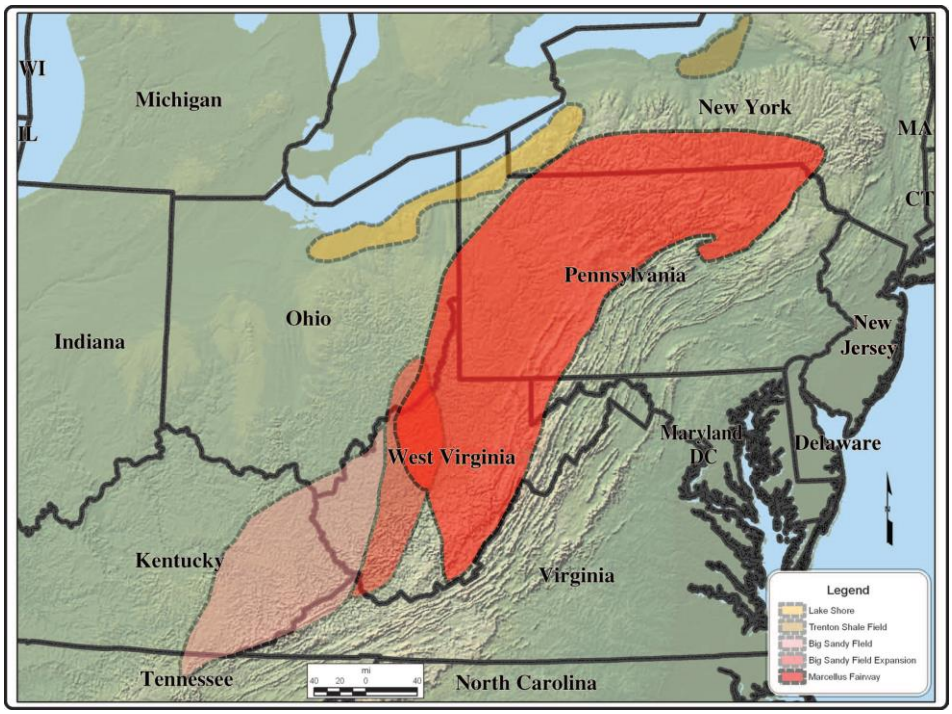

FIGURE 5.1 Marcellus shale play(Zagorzy, Wrighstone and Bowman, 2012)

The information used in this thesis is of public domain and provided generously by Kentucky Geological Survey(KGS).

Appalachi quadrangle is conformed by 12 wells. Information is available only for 9 of the 12 wells conforming the quadrangle. The wells whose information was available produce exclusively gas.

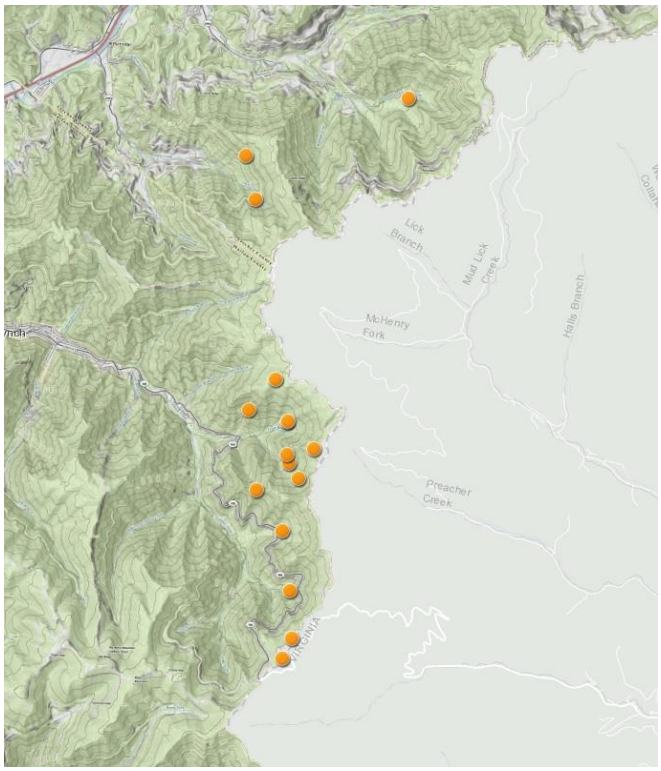

Figure 5.2 Map showing the quadrangle Appalachi, USA.(KGS, 2018)

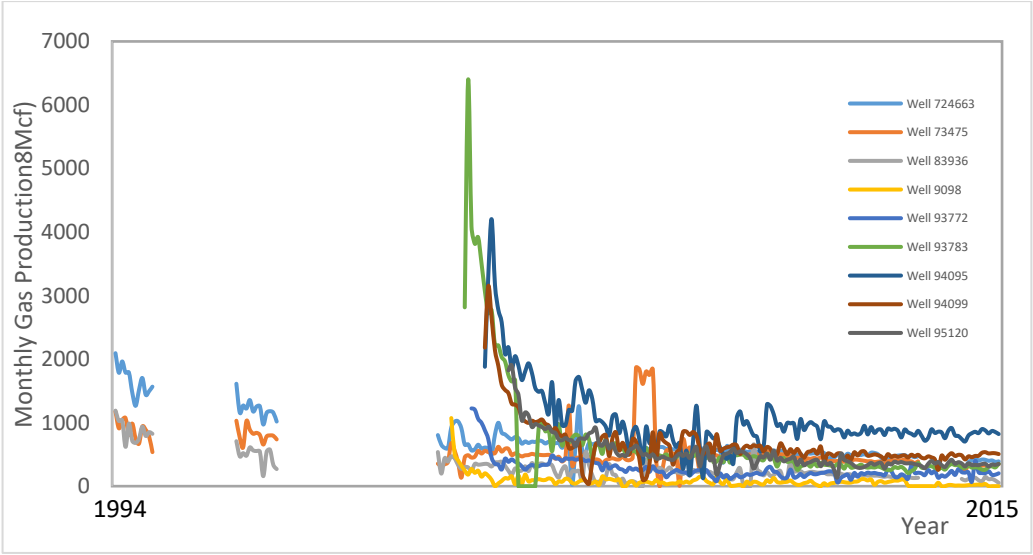

FIGURE 5.3 Historical Production of Appalachi Quadrangle from 1994 to 2015.

5.1 Well 93783.

The production history match and forecast obtained by ST PRO Model is displayed in figure 5.10.

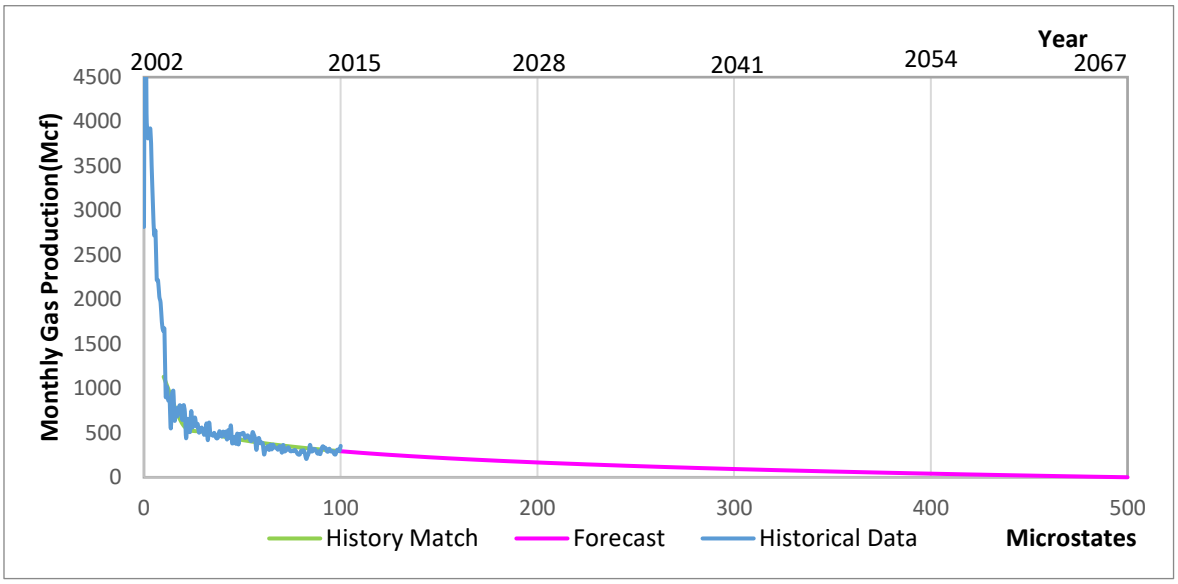

FIGURE 5.10 History match and forecast using ST PRO Model in the well 93783.

The spherical desorption radius squared obtained by ST PRO Model is 89,672$[ft^2]$ (see fig. 5.11) after 17,373 iterations of the ST PRO Model. ST PRO Model performed 10,000,000 Monte Carlo simulations for each ST PRO iteration.

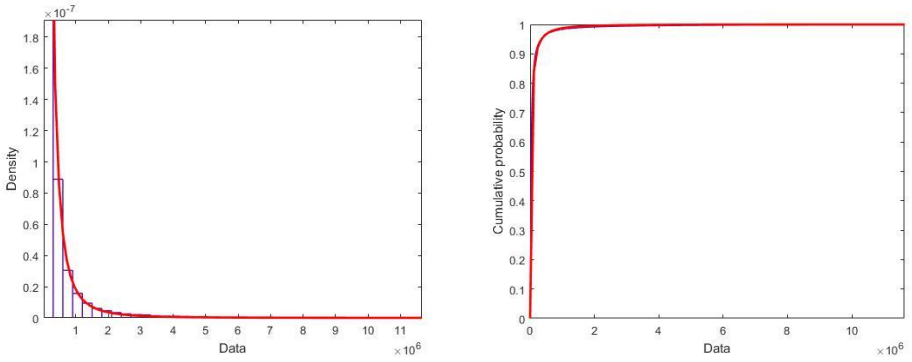

FIGURE 5.11 Left: Lognormal distribution showing the spherical desorption radius squared (mean of the lognormal distribution) of 89,672$[ft^2]$ after 17,373 ST PRO Model iterations. Right: Cumulative distribution function of the lognormal distribution shown on the left side.

The spherical radius of desorption is 299$[ft]$ with a desorption area of 1,123,446 $[ft^2]$.

5.2 Well 73475.

This well has been producing during three different periods of time(see figure 5.3). The well started producing in January 1994. The last production report was in December 2015.

By using ST PRO Model with the historical production data, we were able to find three different patrons during its production. In order to make a full analysis of the production of the well, three different production forecasts were created.

The first production history match and forecast is shown in figure 5.4. The spherical desorption radius squared obtained is 52,028 $[ft^2]$ (See figure 5.5). The historical data was matched after making 10,100 iterations of the ST PRO Model. Each ST PRO Model simulation made 1,000,000 iterations of Monte Carlo simulation.

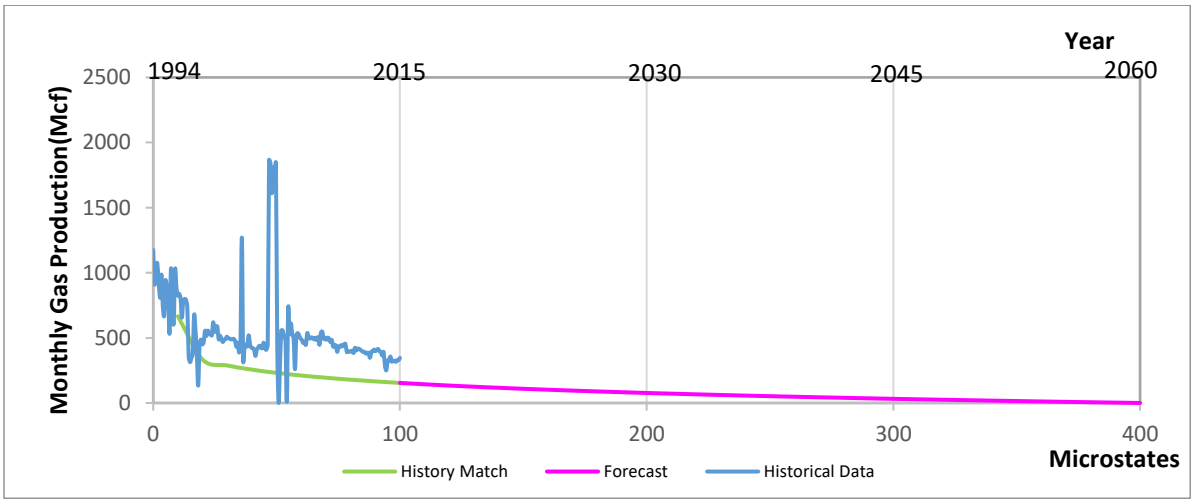

FIGURE 5.4 First history match and forecast using ST PRO Model of well 73475.

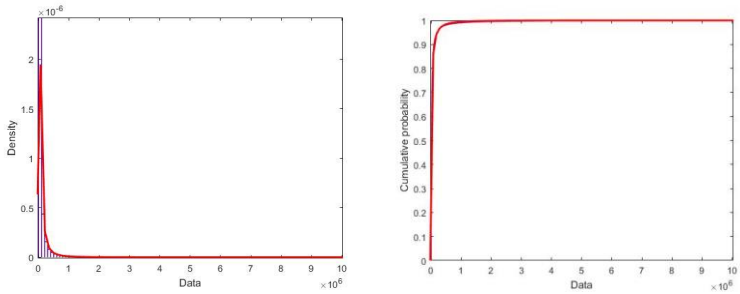

FIGURE 5.5 Left: Lognormal distribution showing the spherical desorption radius squared (mean of the lognormal distribution) of 52,028$[ft^2]$ after 10,100 ST PRO Model iterations. Right: Cumulative distribution function of the lognormal distribution shown on the left side.

The spherical radius of desorption is 228 $[ft]$ with a desorption area of 653250$[ft^2]$.

For the second production history match and forecast calculated by using ST PRO Model is presented in the figure 5.6. It seems the increment in the production was due to natural cracking of organic and inorganic material. The spherical desorption radius squared obtained by ST PRO Model is 93,634$[ft^2]$ (see fig. 5.7). The historical data was matched after making 18121 iterations of the ST PRO Model. Each ST PRO Model simulation made 10,000,000 iterations of Monte Carlo simulation.

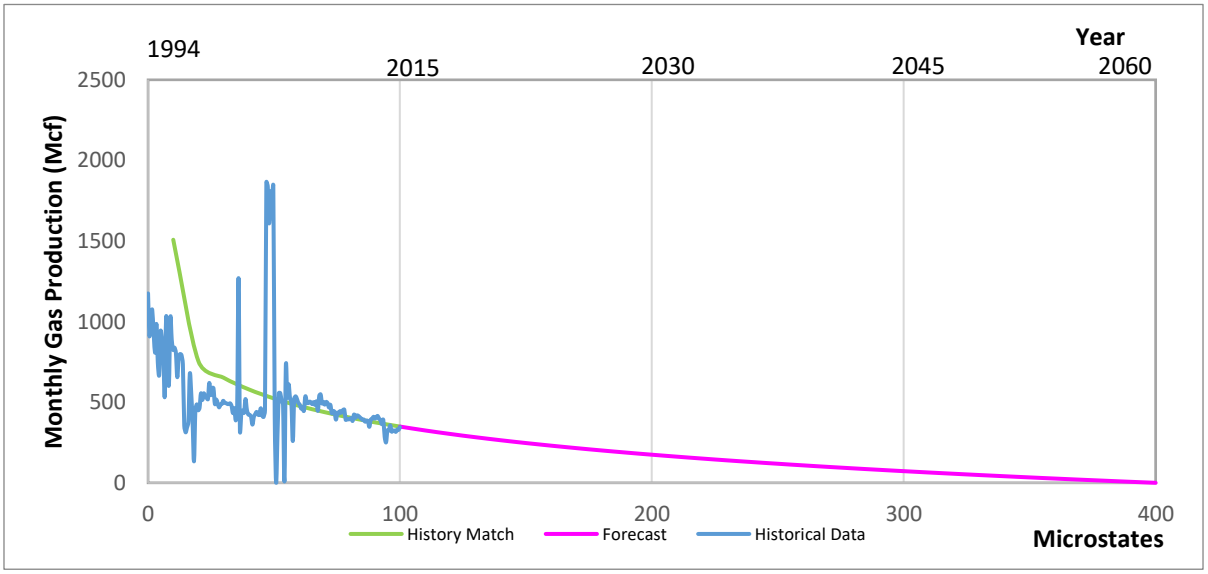

FIGURE 5.6 Second history match and forecast using ST PRO Model of the well 73475.

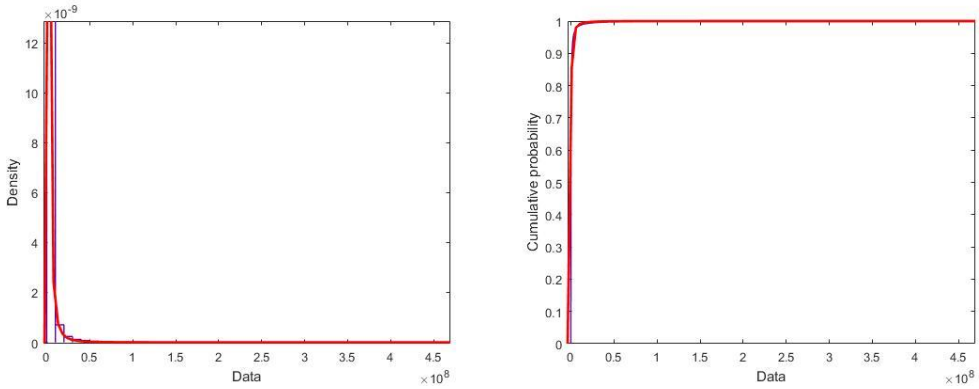

FIGURE 5.7 Left: Lognormal distribution showing the spherical desorption radius squared (mean of the lognormal distribution) of 93,634$[ft^2]$ after 18,121 ST PRO Model iterations. Right: Cumulative distribution function of the lognormal distribution shown on the left side.

The spherical radius of desorption is 306 $[ft]$ with a desorption area of 1,176,664$[ft^2]$.

The third production history match and forecast made by ST PRO Model is shown in figure 5.8. It seems the operator added new production stages into the well. The peak in the gas production profile at the beginning of the third history match could represent the initial free gas being produced. Once all the free gas was produced, the well produced gas uniquely by desorption mechanism. ST Pro Model matched the historical data at this stage and found an spherical desorption radius squared of 123,688$[ft^2]$. The history matching was reach after 23,944 iterations(see fig. 5.9). For this case, 10,000,000 Monte Carlo simulations were perform for each ST PRO Model iteration.

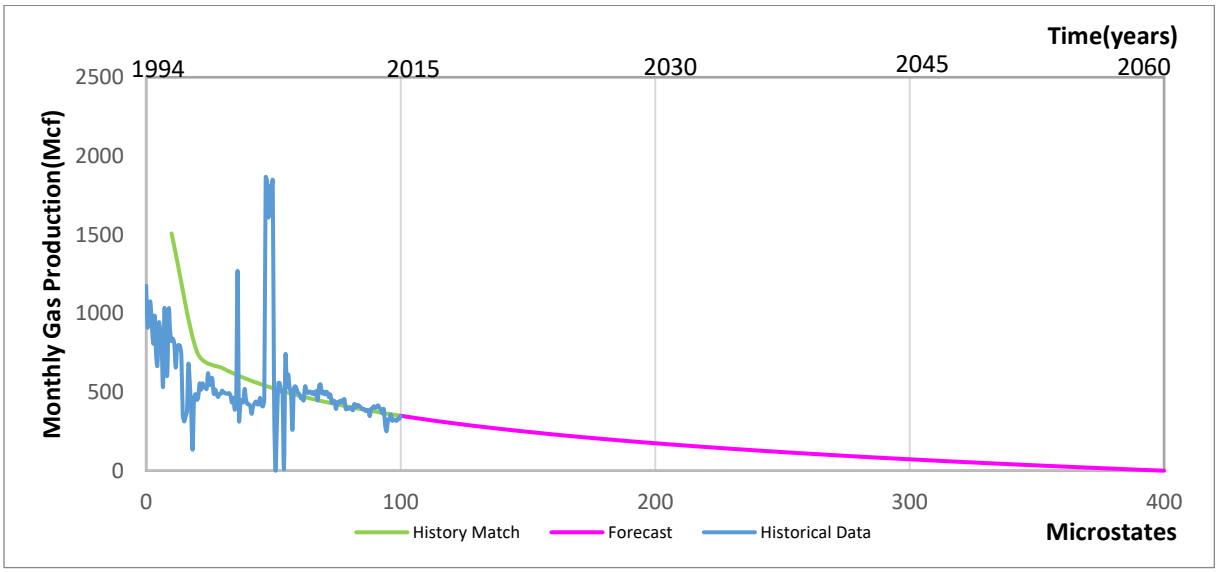

FIGURE 5.8 Third history match and forecast using ST PRO Model of well 73475.

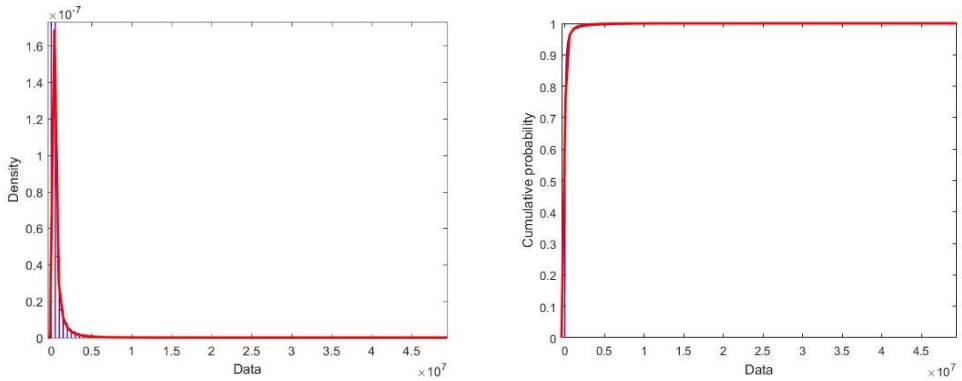

FIGURE 5.9 Left: Lognormal distribution showing the spherical desorption radius squared (mean of the lognormal distribution) of 123,688$[ft^2]$ after 23,944 ST PRO Model iterations. Right: Cumulative distribution function of the lognormal distribution shown on the left side.

The spherical radius of desorption is 351 $[ft]$ with a desorption area of 1,554,309$[ft^2]$.

5.3 Well 94099.

The production history match and forecast obtained by using ST PRO Model is shown in figure 5.12.

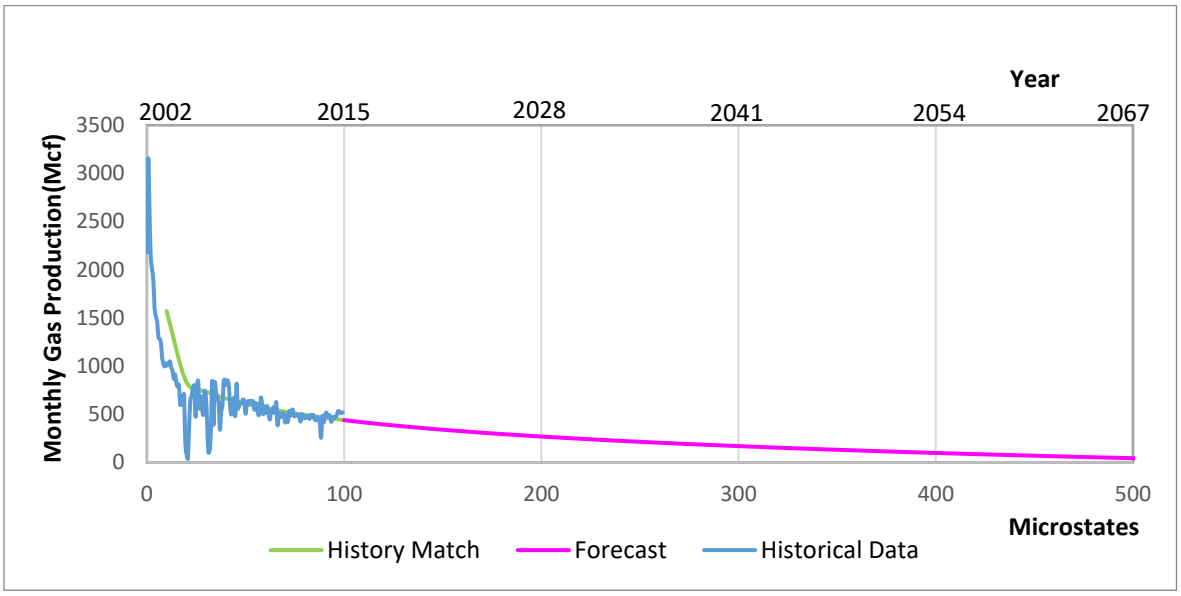

FIGURE 5.12 History match and forecast using ST PRO Model in the well 94099.

ST PRO Model was able to match the historical data after 24,684 iterations. The spherical desorption squared radius obtain by ST PRO Model is 127,493 $[ft^2]$ (see fig. 5.13). ST PRO Model performed 100,000,000 Monte Carlo simulations for each ST PRO Model iteration.

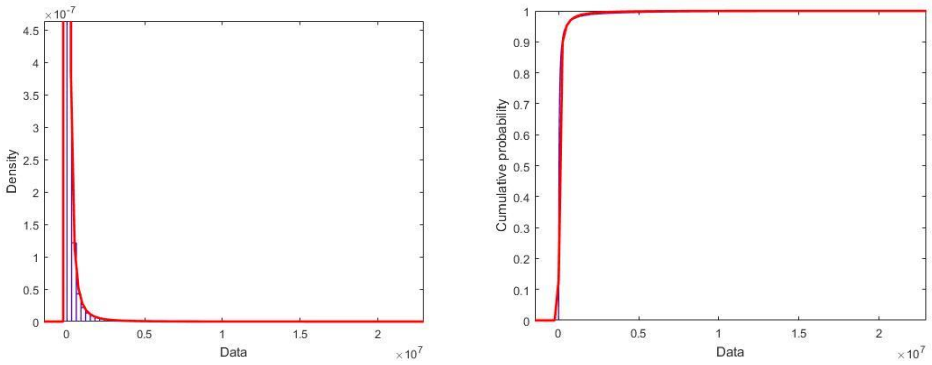

FIGURE 5.13 Left: Lognormal distribution showing the spherical desorption radius squared (mean of the lognormal distribution) of 127,493$[ft^2]$ after 24,684 ST PRO Model iterations. Right: Cumulative distribution function of the lognormal distribution shown on the left side.

The spherical radius of desorption is 357$[ft]$ with a desorption area of 1,602,124$[ft^2]$.

5.4 Well 95120.

The history match and production forecast obtained by using ST PRO Model is shown in figure 5.14.

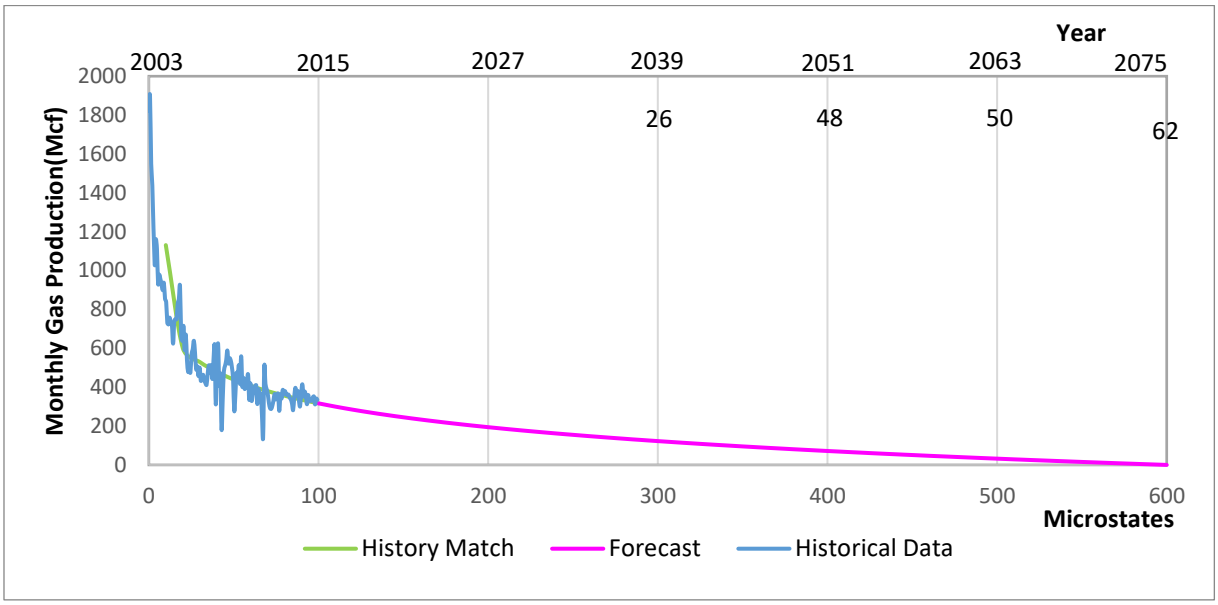

FIGURE 5.14 History match and forecast using ST PRO Model in the well 95120.

ST PRO Model was able to match the historical data after 18,100 iterations. The spherical desorption squared radius obtain by ST PRO Model was 93,297 $[ft^2]$ (see fig. 5.15). ST PRO Model performed 1,000,000 Monte Carlo simulations for each ST PRO Model iteration.

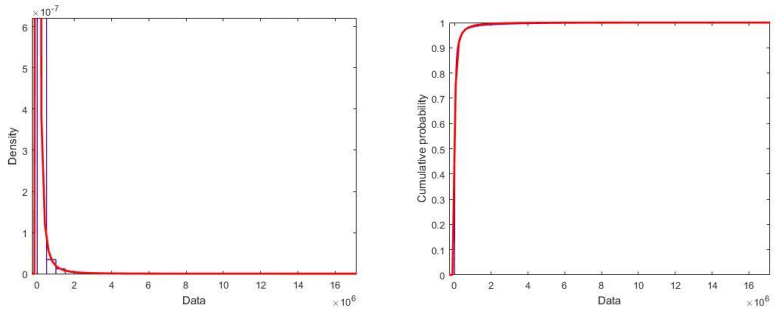

FIGURE 5.15 Left: Lognormal distribution showing the spherical desorption radius squared (mean of the lognormal distribution) of 93,297$[ft^2]$ after 18,100 ST PRO Model iterations. Right: Cumulative distribution function of the lognormal distribution shown on the left side.

The spherical radius of desorption is equivalent to a 305$[ft]$ with a desorption area of 1,172,404$[ft^2]$.

5.5 Three wells producing simultaneously.

The quadrangle Appalachi had an initial well development in 1994. Three wells started production of gas back then(see fig. 5.3). The history match and forecast for the initial development wells is displayed in Figure 5.16.

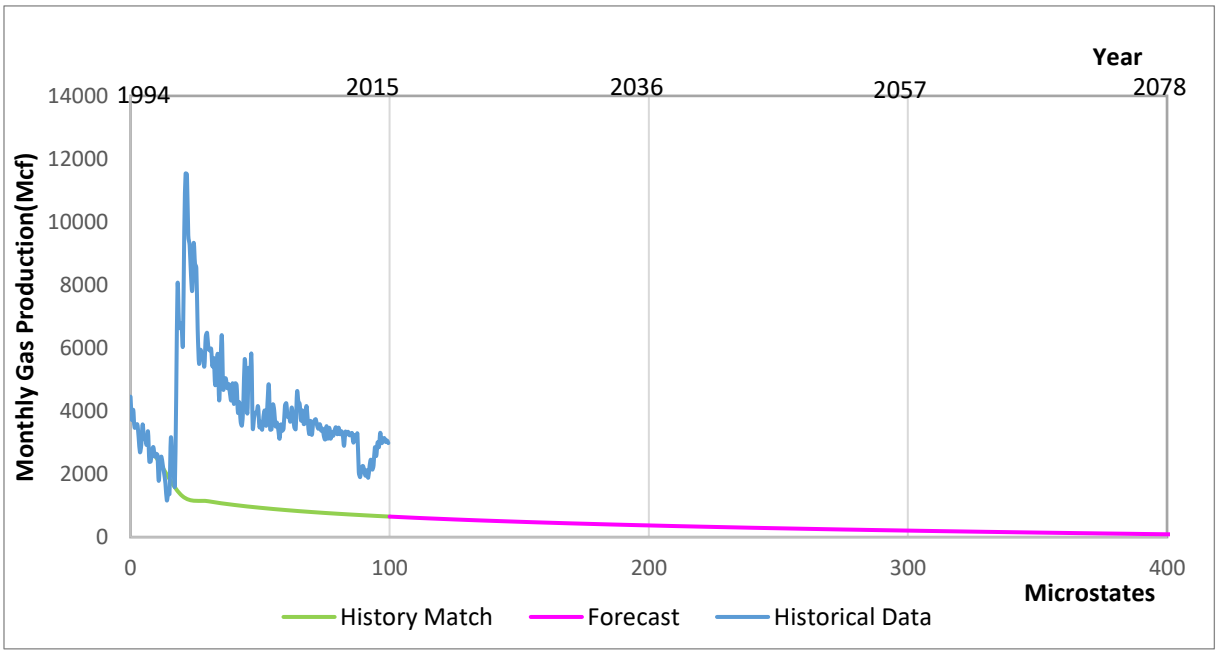

FIGURE 5.16 History match and forecast using ST PRO Model for three production wells open for production in Appalachia quadrangle.

ST PRO Model was able to match the historical data after 38831 iterations. The spherical desorption squared radius obtain by ST PRO Model is 200,532 $[ft^2]$ (see fig. 5.13). ST PRO Model performed 10,000,000 Monte Carlo simulations for each ST PRO Model iteration.

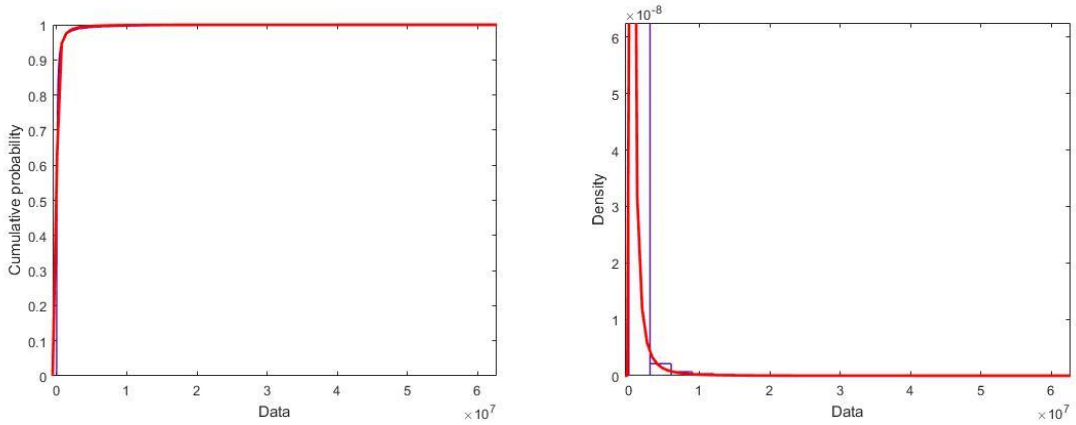

FIGURE 5.17 Left: Lognormal distribution showing the spherical desorption radius squared (mean of the lognormal distribution) of 200,532$[ft^2]$ after 38,831 ST PRO Model iterations. Right: Cumulative distribution function of the lognormal distribution shown on the left side.

The spherical radius of desorption 447$[ft]$ with a total desorption area of 2,519,959$[ft^2]$.

5.6 Nine wells producing simultaneously.

Six additional wells started production in 2002. From 2002 to 2015, nice wells were producing simultaneously. The history match and forecast for group of nine wells is shown in Figure 5.

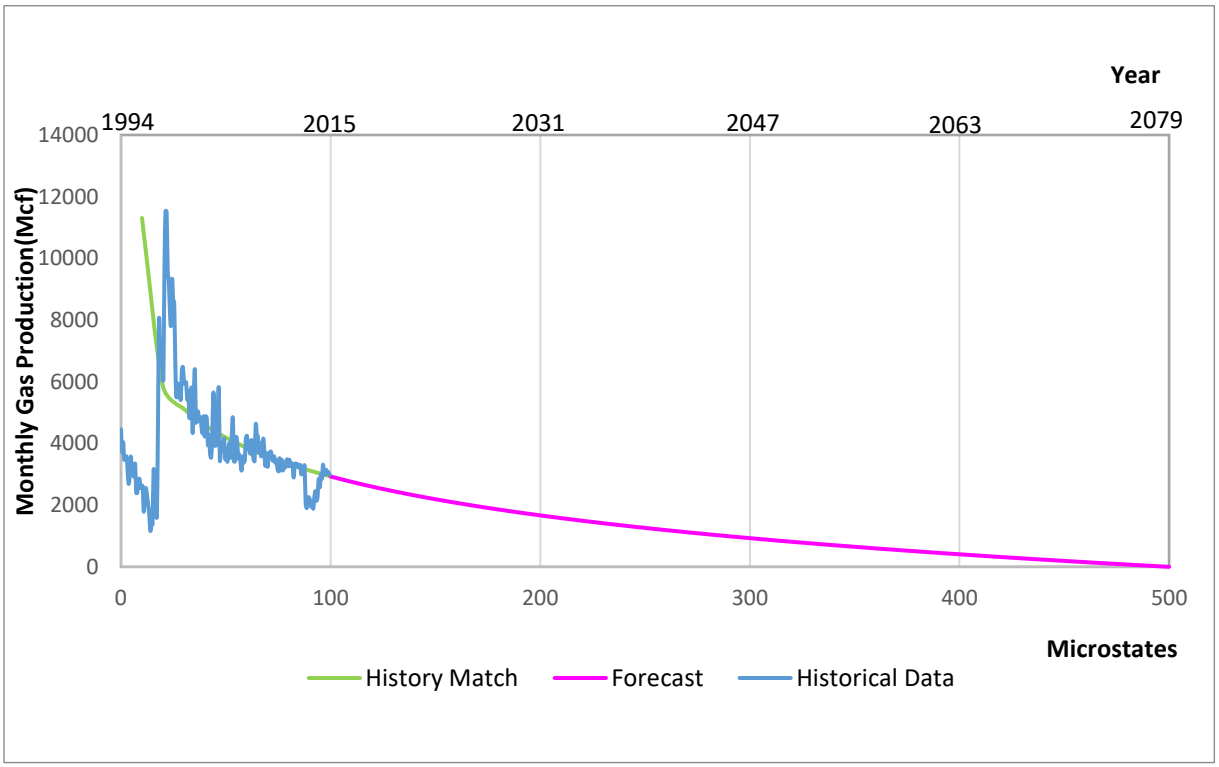

FIGURE 5.18 History match and forecast done by using ST PRO Model for 9 wells open for production in Appalachia quadrangle.

ST PRO Model was able to match the historical data after 179,331 iterations. The spherical desorption squared radius obtain by ST PRO Model is 902,235 $[ft^2]$ (see fig. 5.13). ST PRO Model performed 100,000,000 Monte Carlo simulations for each ST PRO Model iteration.

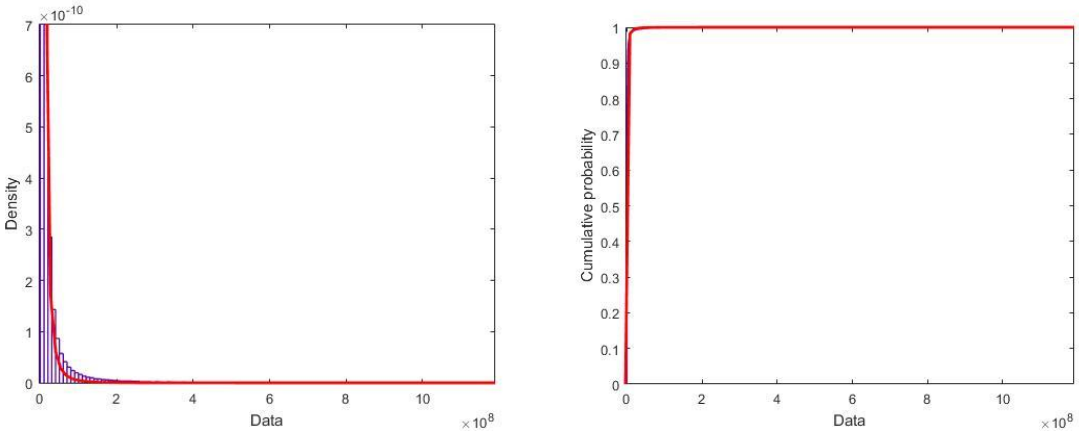

FIGURE 5.19 Left: Lognormal distribution showing the spherical desorption radius squared (mean of the lognormal distribution) of 902,235$[ft^2]$ after 174,331 ST PRO Model iterations. Right: Cumulative distribution function of the lognormal distribution shown on the left side.

The spherical radius of desorption 950$[ft]$ with a total desorption area of 11,337,819$[ft^2]$.

Chapter 6: Conclusions.

This thesis provides a new method (named ST PRO Model) for the forecasting of wells producing gas from shale gas reservoirs. In addition, the model gives a possible value of desorption area inside the reservoir. ST PRO Model is based in a novel analysis by means of a stochastic thermodynamic analysis of the geochemical properties of shale gas.and a stochastic spherical diffusion model. A new adsorption/desorption isotherm named RP isotherm has been formulated. ST PRO Model has been successfully applied in a case study of wells located at the east of Kentucky, USA.

Conclusions:

1. Large desorption areas are due to the microstructural characteristics of the shale gas rock.
2. Description of the production of gas from shale gas reservoirs by the combination of the geochemical properties of the shale gas with *the first and second law of thermodynamic*s.
3. ST PRO Model makes the forecasting of shale gas reservoir based in the thermodynamic properties of the shale gas and spherical desorption surface area quantification.
4. RP isotherm as an alternative of Langmuir isotherm for adsorption/desorption modeling.
6. No pressure data needed for the forecasting of a shale gas well or group of wells.
7. Potential tool for production forecasting of an individual or group of wells.
8. Quantification of a possible desorption area of the induced fracture network by means of a stochastic spherical diffusion model.
9. ST PRO Model can identify, quantify and reforecast an increment in the induced fracture network of a well. The increment in the induced fracture network can be related to a natural process (cracking of organic and non-organic material due to production), or artificially due to addition of new stages or hydraulic fracturing.
10. ST PRO Model can be effectively used for hydraulic fracturing design.
11. ST PRO Model suits as a potential non-empirical tool for forecasting shale gas wells.

NOMENCLATURE

C_t	Concentration at a specific time [1]
C_F	Final concentration [1]
D	Diffusion $\left[\frac{m^2}{s}\right]$
K_b	Boltzmann constant $\left[\frac{m^2 kg}{sK}\right]$
K_{RP}	RP constant $[ft^3]$
P	Pressure $[psia]$
$P_{reservoir}$	Pressure at reservoir conditions $[psia]$
$P_{surface}$	Pressure at surface conditions $[psia]$
Q	Rate of gas $[ft^3/day]$
q	Heat $[J]$
q_{rev}	Heat in a reversible system $[J]$
S	Entropy
S_0	Entropy at initial conditions
T	Temperature $[R]$
$T_{reservoir}$	Temperature at reservoir conditions $[K]$
$T_{surface}$	Temperature at surface conditions $[K]$
U	Internal energy $[J]$
$U_{heat\ source}$	Internal energy of the reservoir's heat source $[J]$
$U_{particles\ of\ gas}$	Internal energy of gas particles in the reservoir $[J]$
V	Volume $[ft^3]$
ΔV	Volume difference $[ft^3]$
V_0	Volume of gas at initial conditions $[ft^3]$
V_a	Volume of gas in point "a" (fig. 3.1) $[ft^3]$
V_b	Volume in point "b" (fig. 3.1). $[ft^3]$
$V_{heat\ source}$	Volume of reservoir's heat source $[ft^3]$
$V_{particles\ of\ gas}$	Volume of particles of gas in the reservoir $[ft^3]$
$V_{reservoir}$	Volume of gas at reservoir conditions $[ft^3]$
$V_{surface}$	Volume of gas at surface conditions $[ft^3]$
w	Work $[J]$
V_F	Final volume of gas produced $[ft^3]$
V_t	Volume of gas at a specific time $[ft^3]$
φ_t	Volume concentration [1]
Ω	Microstates

REFERENCES

"Annual Energy Outlook release, 2018", EIA, 2018.

Behar, F., Jarvie, D., 2013, "Compositional modeling of gas generation from two shale gas resource systems: Barnett Shale(United States) and Posidonia Shale(Germany)", AAPG Memoir 103.

Crank, J., 1975, "The Mathematics of Diffusion", 2nd edition.

Gaskell, D.R. 2003 . "Introduction to the thermodynamics of materials", 4th edition.

Jarvie, D.M., 2015, "Fundamentals of Shale Gas Reservoirs", 1st edition.

King, G.E., 2012, "Hydraulic Fracturing 101: What Every Representative, Enviromentalist, Regulator, Reporter, Investor, University Researcher, Neighbor and Engineer Should Know about Estimating Frac Risk and Improving Frac Performance in Unconventional Gas and Oil Wells", presented at 2012 SPE Hydraulic Fracturing Technology Conference, Feb 6-8, The Woodlands, Texas, USA, SPE 152596.

Kittel,C., 1958, "Elementary Statistical Physics", 1st edition.

Mongalvy, V., Chaput, E., and Agarwal, S., 2011, "A New Numerical Methodology for Shale Reservoir Performance Evaluation", presented at 2011 SPE North American Unconventional Gas Conference and Exhibition, Jun 14-16, The Woodlands, Texas, USA, SPE 144154.
Shaw, G., and Stone, T., 2005, "Finite Volume Methods for Coupled Stress/Fluid Flow in a Commercial Reservoir Simulator", presented at 2005 SPE Reservoir Simulation Symposium, Jan 31-Feb 2, Houston, Texas, USA, SPE 93430.

Sigal, R.F., Deepak, D., Civan, F., 2015, "Fundamentals of Gas Shale Reservoirs", 1st edition.
Swami, V., Clarkson, C.R., Settari, A., "Non Darcy Flow in Shale Nanopores: Do We Have a Final Answer?", presented at 2012 SPE Canadian Unconventional Resources Conference, Oct 30-Nov 1, Calgary, Alberta, Canada, SPE 162665.

Voß, J., 2004, "Some Large deviation Results for Diffusion Processes", Ph.D. Dissertation, Universität Kaiserslautern, Germany.

Wang, F.P., and Reed, R.M., 2009, "Pore Networks and Fluid Flow in Gas Shales", presented at 2009 SPE Annual Technical Conference and Exhibition, Oct 4-7, New Orleans, Louisiana, USA, SPE 124253.

Zagorsky, W.A., Wrighstone, G.R., Bowman, D.C., 2012, "The Appalachian Basin Marcellus gas play: Its history of development, geologic controls on production, and future potential as a world-class reservoir", AAPG Memoir 97.